

# Modelling primary production: multitude of theories, or multitude of languages?

Jozef Skákala<sup>1,2</sup>, Shubha Sathyendranath<sup>1,2</sup>, Yuri Artioli<sup>1</sup>, Deep S Banerjee<sup>1,2</sup>, Heather Bouman<sup>3</sup>, Robert J.W. Brewin<sup>4</sup>, Momme Butenschön<sup>5</sup>, Stefano Ciavatta<sup>6</sup>, Stephanie Dutkiewicz<sup>7</sup>, Yanna Fidai<sup>1</sup>, David Ford<sup>8</sup>, Grinson George<sup>9</sup>, Karen Guihou<sup>6</sup>, Bror Jönsson<sup>10</sup>, Marija Bačekočić Koloper<sup>11</sup>, Žarko Kovač<sup>11</sup>, Lekshmi Krishnakumary<sup>1</sup>, Gemma Kulk<sup>1,2</sup>, Charlotte Laufkötter<sup>12</sup>, Gennadi Lessin<sup>1</sup>, Jann Paul Mattern<sup>13</sup>, Angélique Melet<sup>6</sup>, Alexandre Mignot<sup>6</sup>, David Moffat<sup>1,2</sup>, Fanny Monteiro<sup>14</sup>, Mayra Rodriguez Bennadji<sup>4</sup>, Cécile S. Rousseaux<sup>15</sup>, Ranjini Swaminathan<sup>16</sup>, Osvaldo Ulloa<sup>17</sup> and Jerry Tjiputra<sup>18</sup>

<sup>1</sup>Plymouth Marine Laboratory, UK,

<sup>2</sup>National Centre for Earth Observation, UK,

<sup>3</sup>University of Oxford, UK,

<sup>4</sup>University of Exeter, UK,

<sup>5</sup>Euro-Mediterranean Center on Climate Change (CMCC), Italy,

<sup>6</sup>Mercator Ocean International, France,

<sup>7</sup>Massachusetts Institute of Technology, USA,

<sup>8</sup>Met Office, UK,

<sup>9</sup>Central Marine Fisheries Research Institute, India,

<sup>10</sup>University of New Hampshire, USA,

<sup>11</sup>University of Split, Croatia,

<sup>12</sup>University of Bern, Switzerland,

<sup>13</sup>University of California, Santa Cruz, USA,

<sup>14</sup>University of Bristol, UK,

<sup>15</sup>National Aeronautics and Space Administration (NASA), USA,

<sup>16</sup>University of Reading, UK,

<sup>17</sup>University de Concepción, Chile,

<sup>18</sup>NORCE Research AS, Norway

*Correspondence to:* Jozef Skakala (jos@pml.ac.uk)

**Abstract.** Marine primary production, converting approximately 50Gt of inorganic carbon into organic carbon per year, is an important component of the global carbon cycle, and a major determinant of past, present and future climate. Large-scale, long-term estimates of marine primary production rely primarily on two types of models: satellite-based models that make extensive use of remote-sensing data, and ecosystem models providing numerical simulation of ecological processes embedded in general ocean circulation models. Intercomparison exercises of model outputs (both within and across the two model types) have consistently revealed high discrepancies between estimated global ocean primary production, including divergent magnitudes and even opposite trends. Model-observation comparisons are also complex, because paucity of data, differences in measurement techniques, and evolving methodologies could all lead to difficulties with the interpretation of results. These uncertainties limit the applications of primary production models (both satellite-based and ecosystem), especially in the climate context, where an important question is whether climate change will drive significant future changes in regional or global primary production. Both satellite-based and ecosystem models rely on a range of fixed model parameters, whose values need to be carefully estimated and tested. In this paper, we suggest that such model parameters represent an underappreciated but important source of inter-model differences. With the proliferation

47 of both satellite and *in situ* observations of relevant variables at global scales, and the availability of powerful  
48 statistical tools such as data assimilation and machine learning, we argue that time is right to systematically  
49 examine model parameters, gaining both better insights into parameter values and how those values might vary  
50 in space and time. We argue that such spatio-temporal parameter variability can be theoretically justified for  
51 ecosystem models with complexity similar to those commonly used within Earth System Models (ESMs) in  
52 climate studies. The spatially and temporally varying parameter values could serve to unify models that are  
53 structurally different. An important aspect of this unification could be the ability to infer the spatio-temporal  
54 variability of parameters in the less complex models from the emergent behaviour of the more complex ones. This  
55 could include ecosystem model simulations of nutrients, temperature, phytoplankton classes, or vertical  
56 distributions informing satellite-based models. We conclude that better understanding of model parameter roles  
57 and integration (or inter-calibration) of different types of models could reduce discrepancies among the primary  
58 production models and improve the reliability of marine primary production projections.

59  
60

## 61 **1. Introduction**

62 The climate problem is highly complex, the stakes are very high, and substantial knowledge gaps remain,  
63 especially in the ocean biogeochemistry domain (Kwiatkowski *et al.*, 2020). More broadly, the need to address  
64 complex issues related to the carbon cycle, ecosystem services and biogeochemistry through Earth System Models  
65 (ESMs), e.g., in the context of climate adaptation and resilience, has been highlighted by expert groups (Hewitt  
66 *et al.* 2021). Similarly, Jones *et al.* (2024) evaluate modelling priorities to support international climate policy and  
67 emphasise the value of “a coordinated, internally consistent set of simulations, data, and knowledge to support  
68 Intergovernmental Panel on Climate Change (IPCC) assessments” and outline multiple applications of Coupled  
69 Model Intercomparison Project (CMIP) projections. These include investigations of threats to marine ecosystems  
70 (which have consequences for the ocean’s ability to buffer climate change, Tjiputra *et al.*, 2025) and downstream  
71 services under various climate scenarios and associated risks of tipping points. Jones *et al.* (2024) also state that  
72 improving confidence in future projections requires models to reproduce the observed historical period.  
73 Furthermore, they identify parameter uncertainty as one of the key elements of uncertainty in climate models.

74 Against this background and in line with the recommendations of expert bodies, we focus on the climate  
75 priority challenge associated with marine ecosystem and biogeochemistry modelling, and particularly on marine  
76 primary production. Phytoplankton primary production (PP), the process by which marine autotrophs convert CO<sub>2</sub>  
77 into organic matter through photosynthesis, is a major component of the ocean and planetary carbon cycle.  
78 Currently estimated at around 50 Pg C y<sup>-1</sup> (Kulk *et al.* 2020, 2021), the magnitude of marine PP is five times the  
79 estimated fossil fuel emissions of 10 Pg C y<sup>-1</sup> in 2022 and nearly 20 times the net ocean carbon sink (Friedlingstein  
80 *et al.* 2024). Its magnitude is comparable to that of terrestrial primary production (Lurin *et al.* 1994; Longhurst *et al.*  
81 1995; Field *et al.* 1998; Friedlingstein *et al.* 2024). A key question in climate research is whether the current  
82 levels of marine PP can be maintained under climate change (Tagliabue *et al.*, 2021), when marine ecosystems  
83 are increasingly threatened by a variety of processes, including ocean acidification (Jin *et al.*, 2020, Dai *et al.*,  
84 2025), rising seawater temperatures (Kwiatkowski *et al.*, 2020), intensified storminess over the oceans (Gastineau  
85 and Soden, 2009, Young *et al.*, 2019, Gentile *et al.*, 2023, Liu *et al.*, 2024), ocean deoxygenation (Schmidtko *et al.*  
86 *et al.*, 2017), modified current and stratification influencing surface nutrients (Maishal, 2024), changes in aerial  
87 nutrient supply (Bergas-Masso *et al.*, 2025), biodiversity loss (Luypaert *et al.*, 2020), and sea-ice loss (Mykswoll

88 *et al.*, 2023). In this review we consider PP estimated from two types of models: “satellite-based models” that  
89 utilise remote-sensing data together with physiological models, whose parameters are informed by *in situ*  
90 measurements, to calculate PP; and mechanistic “ecosystem models” which use numerical methods to solve a set  
91 of differential equations representing many ecological processes, with one of them being PP.

92 When discussing marine PP it is important to keep track of its different components. Theoretically, PP before  
93 any of the loss terms are considered is referred to as gross PP (GPP); once the respiration by marine autotrophs is  
94 subtracted from GPP we obtain net PP (NPP). GPP can also be partitioned according to whether only the organic  
95 carbon fixed into particulate material is considered (production of particulate organic carbon), or if the exudates  
96 (dissolved organic matter) are also included in the estimate (production of total organic carbon, Regaudie-de-  
97 Gioux *et al.* 2014). Models can make explicit distinction between these components, though this is not always  
98 done. When it comes to *in situ* observations, experimental methodologies and carefully assembled protocols exist  
99 for measurement of each of these components (IOCCG, 2022); however, practical constraints may limit the extent  
100 to which the components may be differentiated from each other. Furthermore, various observational methods of  
101 the same component could yield differing values. For example, multiple methods for measuring the same  
102 component could have different intrinsic timescales that are applicable to them, making direct comparisons  
103 difficult. Improving observational tools for PP, including developing reliable PP error models, is a priority for the  
104 scientific community, in addition to the modelling issues that are the primary focus of this paper.

105 Here, we focus mainly on GPP as computed in many ecosystem models. For satellite-based estimates, we  
106 treat PP derived from short (1-4 hours) *in situ* incubations as GPP, and those derived from longer (12-24 hour)  
107 incubations as NPP, while fully recognising that the distinction is not that clear cut (e.g., Halsey *et al.*, 2011).  
108 Furthermore, estimates of the magnitude of losses due to respiration vary considerably. Some estimates place it  
109 at about 30% of GPP (e.g., Platt *et al.*, 1991), while some other estimates are higher (e.g., 60% according to Halsey  
110 *et al.*, 2011). Platt and Sathyendranath (1988) compared daily water-column PP computed on the basis of short  
111 incubations with those measured *in situ* over daily time scales, and showed the two sets of independent estimates  
112 to be comparable, which points to low respiration losses. Also, satellite-based estimates of NPP (Behrenfeld and  
113 Falkowski, 1997) tend to be roughly the same or higher than GPP estimates (Longhurst *et al.*, 1995). Since, by  
114 definition, NPP cannot be greater than GPP, these comparisons reveal a great deal of uncertainty in respiration,  
115 or in PP computed using different approaches, when compared with each other.

116

117

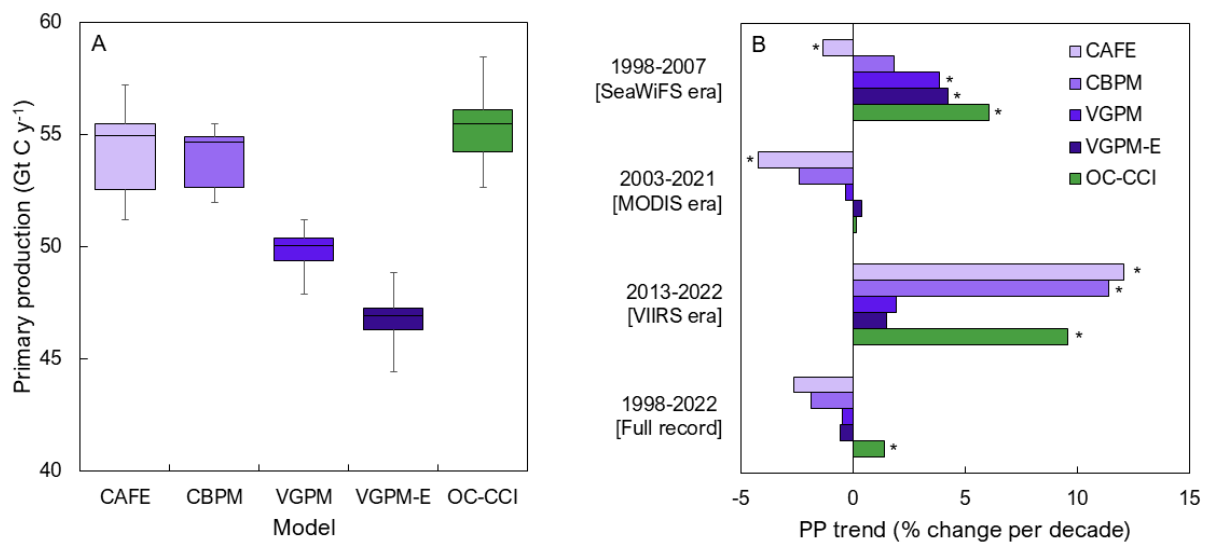
## 118 **2. Background**

119 Considerable differences exist in model-based estimates (here and elsewhere, we use “models” without a  
120 qualifier, to mean both satellite-based and ecosystem models) of the current and past global PP in the ocean, and  
121 in ecosystem-model based projections into the future.

122 Satellite-based estimates of global marine PP are converging around 45-55 Pg C y<sup>-1</sup> (Figure 1A). These  
123 estimates were obtained from both multi-sensor products of the Ocean Colour Climate Change Initiative (OC-  
124 CCI; version 6, Sathyendranath *et al.* 2019, Kulk *et al.* 2020, 2021), as well as from single-sensor products of the  
125 Oregon State University (<http://orca.science.oregonstate.edu/>), which include the Carbon, Absorption, and  
126 Fluorescence Euphotic-resolving (CAFE) model (Silsbe *et al.* 2016; 2025), Carbon-Based Primary Productivity  
127 Model (CBPM; Westberry *et al.* 2008), the Vertically Generalised Production Model (VGPM; Behrenfeld and

128 Falkowski 1997) and the VGPM-Eppley model (which incorporates the Eppley (1972) temperature function).  
 129 However, we note that much higher values (up to 67 Pg C y<sup>-1</sup>) and lower values (≤45 Pg C y<sup>-1</sup>) have also been  
 130 reported from satellite-based products (Antoine *et al.* 1996; Behrenfeld *et al.* 2005; Carr *et al.* 2006; Uitz *et al.*  
 131 2010) (here we recognise that satellite products may differ in the computed PP components, as noted earlier).

132 Large differences also emerge in the PP trends over the last decades estimated from both the CCI and Oregon  
 133 State University products (Figure 1B), as well as associated reanalyses (e.g., those of Gregg and Rousseaux, 2019).  
 134 These differences are strongly impacted by the choice of historical period and the underlying characteristics of  
 135 the satellite products (e.g., single sensor or multi-sensor), but the choice of satellite-based PP model does matter:  
 136 in a recent comparison (Ryan-Keogh *et al.*, 2025) of six satellite-based primary production models applied to a  
 137 common satellite product (OC-CCI) and a common period (1998-2023), four of them showed declining trends,  
 138 while the other two showed an increasing trend. Interestingly, the split is along the lines of whether the models  
 139 incorporated temperature-dependent production parameters, or not. Ryan-Keogh *et al.* (2025) also compared  
 140 satellite products with those of several ecosystem models from the Climate Model Intercomparison Project  
 141 (CMIP-6), and concluded that, in general, the climate models underestimated the decreasing trends seen in some  
 142 of the satellite-based models.  
 143

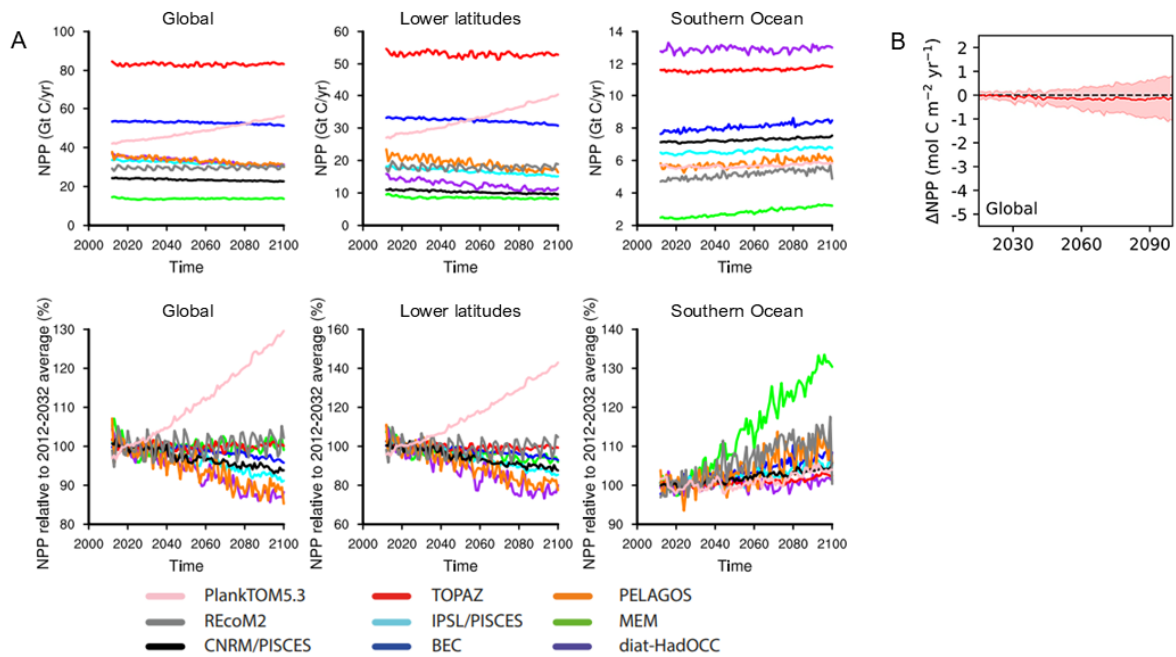


144  
 145 **Figure 1.** Global marine PP computed using the satellite-based model of Platt and Sathyendranath (1988) as  
 146 updated by Sathyendranath *et al.* (2020) and Kulk *et al.* (2020, 2021) with version 6.0 of Ocean Colour Climate  
 147 Change Initiative (OC-CCI) data as input (in green), compared with openly available time-series data from four  
 148 other satellite-based primary production models from the Oregon State University Primary Production website  
 149 ([http://orca.science.oregonstate.edu/-npp\\_products.php](http://orca.science.oregonstate.edu/-npp_products.php)) based on single-sensors: Sea-viewing Wide Field-of-  
 150 view Sensor (SeaWiFS; 1998-2007), Moderate Resolution Imaging Spectroradiometer Aqua (MODIS-Aqua;  
 151 2003-present), and Visible Infrared Imaging Radiometer Suite (VIIRS; 2013-present). The panels show the  
 152 following: A) Global ocean primary production for the five different satellite-based primary production models  
 153 for the time period between 1998-2022 (i.e., full data record), for all sensors combined; and B) Trends in primary  
 154 production for the full ocean colour data record and for subsets of the periods during which specific sensors were  
 155 operational, with stars indicating significant trends ( $p < 0.05$ ), for the five satellite-based primary production  
 156 models. All latitudes were considered, but coverage at higher latitudes ( $>70^{\circ}\text{N}$  and S) is typically poor in satellite

157 data. Differences in marine PP and its trends are not limited to satellite-based products. Earth System Model  
158 intercomparisons show considerably larger uncertainty than the satellite models for the annual NPP estimate  
159 during the (recent past) “historical” period (with values reported in the 17-83 Pg C y<sup>-1</sup> range; Bopp *et al.*, 2013;  
160 Doney *et al.*, 2014; Laufkötter *et al.*, 2015; Tagliabue *et al.*, 2021; see Figure 2), whilst showing weak or no trends  
161 over the recent historical period (Kwiatkowski *et al.*, 2020). Ecosystem model uncertainties are even higher in  
162 future projections where models disagree even on the sign of change up to the year 2100 under the high emission  
163 scenario, although most ecosystem models project a decline in global PP. While the uncertainty in annual NPP in  
164 the recent past has decreased in the CMIP6 (Coupled Model Intercomparison Project phase 6) ensemble compared  
165 with CMIP5, the uncertainty in projected PP trends has increased significantly in the CMIP6 ensemble compared  
166 with CMIP5 (Kwiatkowski *et al.*, 2020). In particular, while the ensemble mean in CMIP5 suggested a significant  
167 decrease in PP at the global scale of  $-8.06\% \pm 4.83\%$  (where the uncertainties are reported as the inter-model  
168 standard deviation), the CMIP6 ensemble has a much smaller mean and the larger standard deviation includes the  
169 null hypothesis of no trend ( $-1.76\% \pm 9.01\%$ ). Frölicher *et al.* (2016) have noted that ecosystem model  
170 uncertainties (missing/mis-represented processes, parameter uncertainties) dominated the total uncertainty in the  
171 21<sup>st</sup>-century projections of PP and their relative importance with respect to scenario uncertainty does not decrease  
172 with projection lead time. Recent studies have confirmed this, highlighting the role of uncertainty in the  
173 representation of key biogeochemical processes, including diazotrophy (Tagliabue *et al.*, 2021; Bopp *et al.*, 2022;  
174 Doléac *et al.*, 2025), bacterial remineralisation (Kim *et al.*, 2023) and parameter uncertainty (Jones *et al.*, 2024),  
175 including in zooplankton grazing rates (Rohr *et al.*, 2023). Laufkötter *et al.* (2015) concluded that the projected  
176 future changes in marine PP are driven by multiple processes, including changes in circulation or mixing, leading  
177 to a stronger lateral or vertical loss of biomass; increased aggregation or mortality of phytoplankton; or higher  
178 grazing pressure. Laufkötter *et al.* (2015) also noted that temperature-dependent functions of PP and loss terms  
179 can affect the direction of change of PP from marine ecosystem models in climate warming scenarios. Regional  
180 variations in PP are especially sensitive to how models represent this wide range of processes (Dutkiewicz *et al.*,  
181 2013), and given the high uncertainty in their model representation, very few of the models agree on the direction  
182 of the trend regionally. Furthermore, global models, with their coarse horizontal resolution, struggle to capture  
183 coastal and estuarine processes that enhance PP (coastal regions account for 14-33% of global PP; Gattuso *et al.*,  
184 1998), which makes them also prone to underestimate global PP.

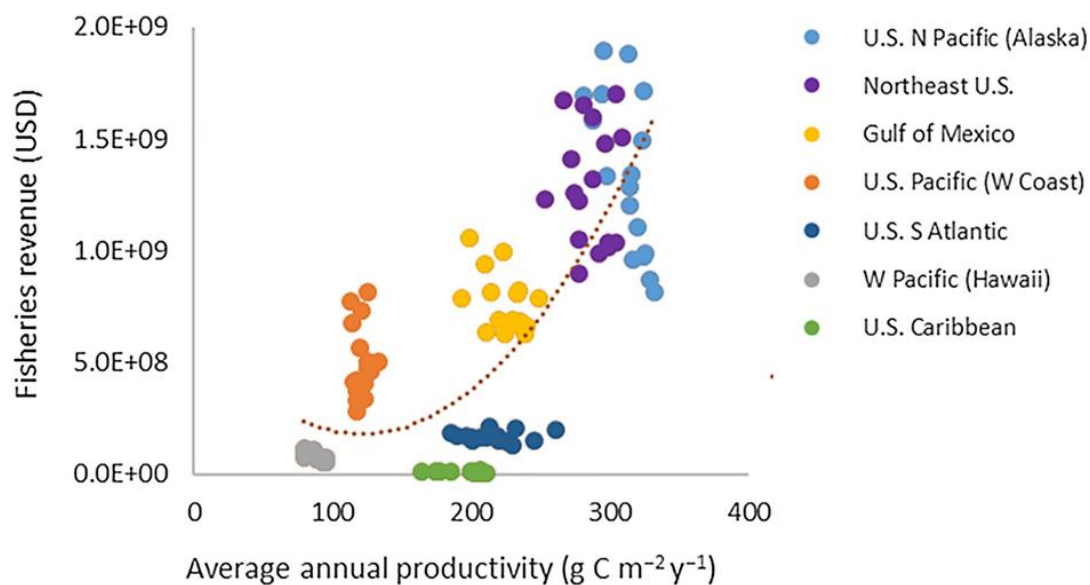
185

186



187  
188  
189  
190  
191  
192  
193  
194  
195  
196  
197  
198

**Figure 2.** Comparison of NPP from marine ecosystem models in CMIP5 comparison projected to the end of this century under a high emission scenario. A) From Laufkötter et al. (2015) – RCP8.5 (Representative Concentration Pathways 8.5 scenario), from left to right are global values, lower latitudes (30°S-30°N) and Southern Ocean (90-50°S) in Gt C per year (top) and percent (bottom); and B) Global NPP projections from Tagliabue et al. (2021) – SSP5-8.5 (Shared Socio-economic Pathways 8.5 scenario). Note that the magnitude of contemporary annual NPP ranges from less than 20 to more than 80 Pg C y<sup>-1</sup> in the compilation from Laufkötter et al. (2015). Both analyses showed negative and positive global trends, though most ecosystem models predict decreasing trends towards the year 2100.



199  
200  
201

**Figure 3.** The impact of PP on fisheries. Figure reproduced from Marshak and Link (2021). Individual observations from different coastal regions of the USA are indicated in different colours.

202 Several studies have also been carried out to compare estimates from ecosystem models with satellite-based  
203 products and *in situ* observations, both at global scale (Carr *et al.*, 2006; Steinacher *et al.*, 2010; Bopp *et al.*, 2013;  
204 Laufkötter *et al.*, 2015; Séférian *et al.*, 2020; Ryan-Keogh *et al.*, 2025) and at regional scales (Friedrichs *et al.*,  
205 2009; Saba *et al.*, 2010; Lee and Yoo, 2016; Doléac *et al.*, 2024). In some cases, these comparisons (e.g., between  
206 ecosystem and satellite-based models) led to better constrained PP projections, e.g., in the tropics, using an  
207 emergent constraint approach (Kwiatkowski *et al.*, 2017). However, it is fair to say that, overall, these comparisons  
208 have not led to convergence of model outputs that would reduce the uncertainty of marine PP estimates. All  
209 previous works have highlighted large differences between estimates (e.g., varying from <-60% to >60%; Séférian  
210 *et al.*, 2020), with highly variable spatial patterns (Bopp *et al.*, 2013). Tagliabue *et al.* (2021) highlighted the need  
211 for stronger constraints on NPP using new approaches that include the growing observational coverage from  
212 Biogeochemical-Argo (BGC-Argo) floats (Claustre *et al.*, 2020; for an example of this see Arteaga *et al.*, 2022).  
213 Field-based observations of PP, typically treated as the “truth”, are often compared with model outputs to evaluate  
214 model performance. However, this type of comparison is confounded by uncertainties in PP measurements, which  
215 can be quite high, as well as by the differences in the spatial and temporal scales of the *in situ* observations and  
216 the validated models. Furthermore, there are also questions around whether the PP is measured directly, or  
217 estimated indirectly. For example, BGC-Argo estimates PP indirectly, inferring it from other, more directly  
218 measured variables.

219 Given these challenges both in remote sensing and ecosystem modelling, the IPCC has assigned low  
220 confidence to current estimates of marine PP and its trends. The reasons cited include uncertainties in production  
221 estimates and projections, the short duration of available time series data used in the analyses, and the lack of  
222 independent validation (IPCC 2019; Gulev *et al.*, 2021; Chapter 2 in IPCC AR6, WG I, 2021). This assessment  
223 is of particular concern as it has major implications for ecosystem service provision, mitigation planning,  
224 enhancing adaptation and building resilience to climate change (Hewitt *et al.*, 2021). These applications often  
225 require regional to local information, as PP determines spatial variability in ecosystem services such as fisheries  
226 (Marshak and Link, 2021; see Figure 3), but uncertainties increase at these scales compared with global estimates  
227 (Tagliabue *et al.*, 2021). Both remote sensing and ecosystem models can, in principle, deliver such regional  
228 insights, when used with granularity and resolution needed at the appropriate scales. Reducing uncertainty in  
229 models, ideally through a coordinated and internally consistent set of simulations, data and knowledge, would  
230 then enable us to discuss downstream services under various climate scenarios and associated risks of tipping  
231 points (Jones *et al.*, 2024). Such improvements would support climate policy, as well as management decisions  
232 pertaining to climate mitigation and adaptation strategies, at both international and regional levels.

233 We argue here that efforts to reduce uncertainty in estimates and projections of marine PP should include a  
234 focus on *investigating model structures and parametrisations*, with the goal of identifying genuine inter-model  
235 differences and reconciling apparent differences. In this review, we examine both the sources of differences  
236 between satellite-based and ecosystem models, as well as within these two types of models. We argue that there  
237 is strong scientific justification for considering how the current model parameterisations could be improved. A  
238 straightforward avenue to improvement is that parameters which are currently treated as constants (e.g., the  $A_i$   
239 parameters from Table 1) are assigned the most appropriate values consistent with the model structure and with  
240 all the available information. A step further is to allow the currently constant parameter values to vary with spatial  
241 locations and times. Although variable parameters would increase the complexity of the functional forms used in

242 PP models, we argue that, at least in the less complex PP models (e.g., within satellite models and ecosystem  
243 models used in ESMs for climate projections), there are good scientific reasons to expect such parameter variations  
244 to be realistic. We propose that absence of such variations is responsible for the many apparent differences  
245 between the current PP models. Parameter variability might be less important for the more complex models with  
246 large numbers of phytoplankton types and/or size-classes, but for those models it is still essential to focus on the  
247 best possible ways of optimising the existing constant parameters. Furthermore, these highly complex models  
248 could provide valuable information for estimating the spatio-temporal variability of parameters used in less  
249 complex ecosystem and satellite-based models. This would also help increase consistency among different  
250 models, making them more comparable. At the same time, caution must be applied to ensure that increased  
251 consistency and convergence is not confused with increased accuracy. For this, we would need to continue  
252 independent assessments of accuracy, for example by comparisons with *in situ* observations, with full recognition  
253 of the caveats that such comparisons entail, as discussed above.

254 In general, we highlight the importance of correct parameterisations that are valid across multiple spatial and  
255 temporal scales, and for multiple phytoplankton types. We also discuss the challenges posed by such PP model  
256 parameterisations, argue that this is the right time to rise to those challenges, and propose strategies to overcome  
257 them. Finally, we discuss uncertainties in marine PP that might persist even when improved model  
258 parameterisations are adopted.

259

### 260 3. Modelling primary production

261 In this section, we assess how marine PP is treated in satellite-based and ecosystem models, identifying inter-  
262 model differences.

263 It is useful to consider GPP as the product of a biomass-specific production, say  $P^M$ , where  $M$  is a measure  
264 of phytoplankton biomass, multiplied by the biomass itself. In other words:

$$265 P = P^M \times M, \quad (1)$$

266 such that  $P^M$  carries all the information on the physiological controls on PP, whereas  $M$  accounts for the role of  
267 varying phytoplankton concentrations. Since phytoplankton are complex organisms, many options exist for  
268 defining biomass, including concentrations of the phytoplankton pigment chlorophyll-a ( $B$ ), phytoplankton carbon  
269 ( $C$ ), or nitrogen content. The choice of biomass often depends on practical considerations (such as data  
270 availability) or by the study objectives (for example, carbon is an obvious choice in models designed to investigate  
271 the biologically mediated carbon cycle in the ocean). Models can also be classified according to which measure  
272 of biomass they track as the main currency in the ecosystem.

273 Dimensional analysis suggests that, in its simplest form,  $P^M$  can be represented in a canonical form with two  
274 parts: a scale factor  $P_m^M$  that carries the same dimensions as  $P^M$ , and a dimensionless function  $f_I$  of the scaled  
275 irradiance  $I_*$  available for photosynthesis (Platt and Sathyendranath, 1993), where the scaling factor would be a  
276 model parameter with the same dimensions as light, such that  $I_*$  is dimensionless. Thus, in such a canonical form,  
277  $P^M$  can be written as:

$$278 P^M = P_m^M \times f_I(I_*). \quad (2)$$

279 In this form,  $P_m^M$  is not strictly constant, but implicitly accounts for the effects of other environmental variables  
280 on primary production, such as temperature ( $T$ ) and nutrients ( $N$ ), or changes in species composition. Such

281 dependencies can be made more explicit (removing  $T$  and  $N$  dependence from  $P_m^M$ ), such that Equation (1)  
282 becomes:

$$283 \quad P^M = P_m^M \times F(f_T(T), f_N(N), f_I(I_*)). \quad (3)$$

284 The function  $F(f_T, f_N, f_I)$  can be specified as a simple product  $f_T \times f_N \times f_I$  (e.g., Laufkötter *et al.*, 2015; Kishi  
285 *et al.*, 2006; Vichy *et al.*, 2007; Yool *et al.*, 2013; Butenschön *et al.*, 2016), representing co-limitation by each  
286 variable, or it can follow Liebig's law of the minimum (e.g., Gregoire *et al.*, 2008; Daewel and Schrum, 2013;  
287 Radtke *et al.*, 2019), where the most limiting resource dictates the growth rate. Note that in Equations 2 and 3, the  
288 functions  $f_i$  are dimensionless, and that all the dimensions are carried by the scaling factor  $P_m^M$ . When models  
289 resolve multiple phytoplankton groups or species, Equation 3 is specified for each group, and their contributions  
290 are added to get total PP.

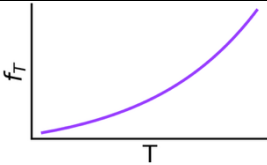
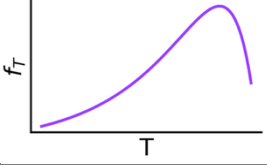
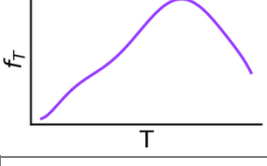
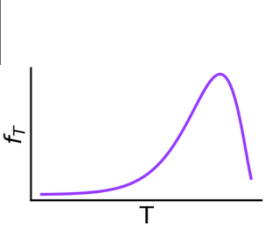
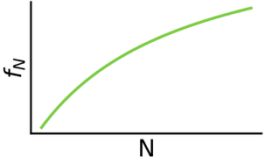
291 Commonly-used functions in PP models that represent the modulating roles of temperature, nutrients and  
292 light are summarised in Table 1. When more than one nutrient is considered, additional terms have to be included  
293 for each nutrient. Thus, models (the combined functions  $F$ ) differ depending on (i) how many environmental  
294 factors are included in the model, (ii) the explicit functional forms selected for each modulating function; and (iii)  
295 the parameter values  $A_i, D_i$  assigned to those modulating functions, and whether they are allowed to vary with  
296 region and time. Finally, the functions  $f_i$  would ideally have values within the  $[0,1]$  interval; however, this is often  
297 not the case for some of the temperature  $f_T$  functions (as can be seen in Table 1).

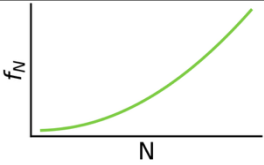
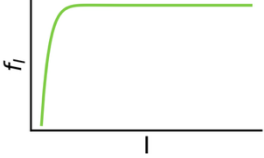
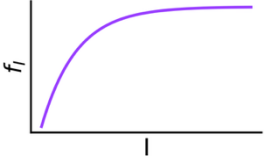
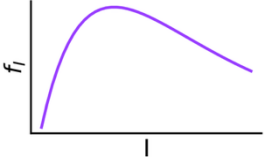
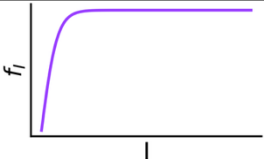
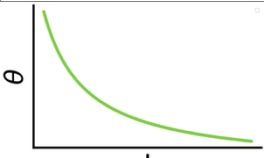
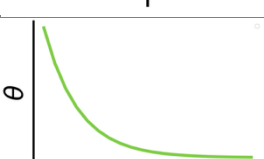
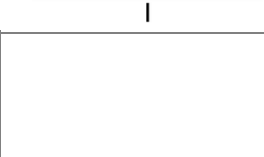
298 In some cases, it is necessary to track multiple measures of phytoplankton biomass within a model. For  
299 example, a unit conversion between chlorophyll-a and carbon might be needed to make the exponent in the light  
300 function ( $f_I$ ) dimensionless, or it may be that the model tracks more than one currency. Such a conversion may  
301 also be needed to transform modelled phytoplankton carbon fields into chlorophyll-a fields for comparison with  
302 satellite-based chlorophyll-a products. This is typically achieved using a chlorophyll-to-carbon ratio ( $\theta$ ), which  
303 varies among phytoplankton and under different environmental conditions and is usually estimated using photo-  
304 acclimation models. Commonly used functions in photo-acclimation models are also shown in Table 1.

305

306 **Table 1.** The different  $f_T, f_N, f_I$  and  $\theta$  functions used across variety of CMIP and operationally used ecosystem  
307 models, as well as satellite models (which however typically do not use an explicit nutrient-limitation function,  
308 see Westberry *et al.*, 2008). The ecosystem models explicitly mentioned are Biogeochemical Model for Hypoxic  
309 and Benthic Influenced areas (BAHMBI; Gregoire and Soetaert, 2010), Biogeochemical Flux Model (BFM; Vichi  
310 *et al.*, 2015), ECOSystem MOdel (ECOSMO; Daewel and Schrum, 2013), European Regional Seas Ecosystem  
311 Model (ERSEM; Butenschön *et al.*, 2016), Hadley Centre Ocean Carbon Cycle (HadOCC; Totterdell, 2013),  
312 Model of Ecosystem Dynamics, Sequestration and Acidification (MEDUSA; Yool *et al.*, 2013), Marine  
313 Ecosystem Model (MEM; Shigemitsu *et al.*, 2012), North-Pacific Ecosystem Model for Understanding Regional  
314 Oceanography (NEMURO; Kishi *et al.*, 2007), PELAgic biogeochemistry for Global Ocean Simulations  
315 (PELAGOS; Vichi *et al.*, 2007), Pelagic Interactions Scheme for Carbon and Ecosystem Studies (PISCES;  
316 Aumont *et al.*, 2015), Carbon, Ocean Biogeochemistry and Lower Trophics (COBALT; Stock *et al.*, 2020, 2025),  
317 and DARWIN model (Ward *et al.*, 2012).  $P_h$  and  $N$  represent the concentrations of phosphate and nitrogen,  
318 respectively. Carbon is represented as  $C$ , and  $A_i$  and  $D_i$  stand for the different model parameters. In  
319 photoacclimation models,  $\theta$  is the chlorophyll-to-carbon ratio.

320

Process / Structure	Equation	Description & remarks	Graphical Representation	Examples	Key References
Temperature limitation on photosynthesis	$f_T = e^{A_1 T}$	Exponential temperature dependence on growth rate.		BAHMBI, MEDUSA, NEMURO, BFM, PISCES, PELAGOS, COBALT, DARWIN	Eppley (1972)
	$f_T = Q_{10} \frac{T-A_2}{A_2} - Q_{10} \frac{T-A_3}{A_4}$	Phytoplankton growth rate increases initially exponentially, with enzyme inhibition above optimal temperature		ERSEM	Blackford <i>et al.</i> (2004)
	$f_T = \sum_{i=0}^7 D_i T^i$	Phytoplankton growth rate is represented as an empirical seventh-order polynomial function, fit to observed data.		Vertically Generalised Production Model (VGPM)	Behrenfeld & Falkowski (1997)
	$f_T = A_5 \times e^{A_6 \times T} \times \left(1 - \frac{T-A_7}{A_8}\right)^2$	Function designed to model individual phytoplankton species or types according to their temperature traits, in multi-species models. It has yet to be used routinely in global-scale simulation models, except in a special case of DARWIN.		A version of DARWIN	Norberg (2004), Thomas <i>et al.</i> (2016); Sauterey <i>et al.</i> 2024); Krinos <i>et al.</i> (2025)
	N/A	No explicit temperature dependence is included in the model structure	N/A	ECOSMO, HadOCC	Yumruktepe, Samuelsen, Daewel (2022)
	Empirical assignment	Indirect methods. An example is province-based assignment of parameters	N/A	Satellite P&S, BICEP	Sathyendranath & Platt (1988), Longhurst <i>et al.</i> (1995), Sathyendranath <i>et al.</i> (2020), Kulk <i>et al.</i> (2020)
N-limitation	$f_N = \left( \frac{\left(\frac{P}{C}\right) - A_9}{A_{10} - A_9} \times \left( \frac{\left(\frac{N}{C}\right) - A_{11}}{A_{12} - A_{11}} \right)^{0.5} \right)$	Describes nutrient limitation based on internal nutrient quota for phytoplankton cells. Droop model of cell quota. $0 \leq f_N \leq 1$ depends on the instantaneously calculated internal cell C/N and C/P ratios $\left(\frac{P}{C}, \frac{N}{C}\right)$ and the maximum C/N and C/P ratios ( $A_5, A_7$ ), having subtracted the structural content of the cell ( $A_4, A_6$ ) from each.	N/A	ERSEM PISCES (for iron), DARWIN (quota version)	Droop (1974);
	$f_N = \frac{N}{N + A_{13}}$	Michaelis-Menton Equation. Describes N-limitation as a saturating function of external nutrient concentration, and the		NEMURO, ECOSMO, BFM, MEDUSA, HadOCC PISCES (for all nutrients except iron),	Michaelis and Menton (1913), Kovarova-Kovar and Egli (1998), Lee <i>et al.</i> (2015)

		half saturation coefficient $A_{13}$ for that nutrient		DARWIN (monod version)	
	$f_N = \frac{(1-f_A) \times A_{14} \times N}{\left(\frac{(1-f_A) \times A_{14}}{f_A \times A_{15}} + N\right)}$ $f_A = \frac{1}{1 + \sqrt{\frac{A_{14} \times N}{A_{15}}}}$	Optimal uptake kinetics		MEM	Smith <i>et al.</i> (2009)
Light Limitation	$f_I = I \times e^{1-A_{16} \times I}$	Photosynthesis rate increases then declines at high light intensities due to photoinhibition.		NEMURO	Steele (1962)
	$f_I = (1 - e^{-A_{17} \times I})$	Photosynthesis follows a light saturation curve with no inhibition at high light levels		Satellite	Platt <i>et al.</i> (1980; 1990) Sathyendranath <i>et al.</i> (2020); Kulk <i>et al.</i> (2020)
	$f_I = (1 - e^{-A_{18} \times I}) \times e^{-A_{19} \times I}$	Photosynthesis follows a light saturation curve with inhibition at high light levels.		BAHBI, MEM	Platt <i>et al.</i> (1980)
	$f_I = \tanh(A_{20} \times I)$	Model with no photoinhibition. A hyperbolic tangent function is used to simulate light saturation curve.		ECOSMO	Jassby & Platt (1976)
Photo-acclimation	$\theta = \frac{A_{21}}{\left(1 + \frac{A_{21} A_{22} I}{2A_{23}}\right)}$	Photo acclimation model based on the concept of resource allocation, with maximum Chl-to-carbon ratio reached as light approaches zero.		ERSEM, BFM, PISCES, PELAGOS, COBALT, DARWIN	Geider <i>et al.</i> (1997,1998)
	$\theta = 0.022 + (0.045 - 0.022)e^{-3I} - g(N, T)$	The Chl-to-carbon ratio ( $\theta$ is determined by photoacclimation, and also by nutrient and temperature stress.		CBPM	Westberry <i>et al.</i> (2008)
	$\theta = \frac{A_{25}}{I \times A_{24}^{-1}} \times \left(1 - e^{-(I \times A_{24}^{-1})}\right)$	Based on an extended version of Geider <i>et al.</i> (1997,1998) photoacclimation model. Uses the exact analytic solution to the Guider <i>et al.</i> (1997) model Jackson <i>et al.</i> (2017), extended to to account for spectral light effects (Sathyendranath <i>et al.</i> 2020). It incorporates photo-acclimation effects on the chlorophyll-to-carbon ratio		Satellite	Sathyendranath <i>et al.</i> (2020), Jackson <i>et al.</i> (2019), Zheng <i>et al.</i> (2025)

322 In the next two sections, we examine in more detail the variety of ways in which these concepts are implemented  
323 in satellite-based and ecosystem models.

324

### 325 3.1 Satellite-based models

326 In satellite-based PP models, daily water-column production is calculated as a function of phytoplankton biomass  
327 and light available at the sea surface, obtained from ocean-colour remote-sensing observations, coupled with  
328 models of photosynthetic response to light. Since the launch of the first ocean-colour satellite, the Coastal Zone  
329 Color Scanner (CZCS) in the 1970s, scientists have developed various satellite-based PP models that can be  
330 roughly categorised into three classes: 1) Chlorophyll-based models, 2) Absorption-based models, and 3) Carbon-  
331 based models (Figure 4). Each of these models could be further classified according to whether they are  
332 implemented as linear/non-linear, spectral/non-spectral, vertically-uniform/vertically-non-uniform, or as a  
333 combination of these (Platt and Sathyendranath, 1993; Sathyendranath and Platt, 2007). Further bifurcations  
334 occur, depending on whether the models are depth-integrated, or not (Friedrichs *et al.*, 2009). Most of the satellite-  
335 based models do not resolve PP by phytoplankton size classes, or functional types, with some exceptions, such as  
336 Uitz *et al.* (2010), Brewin *et al.* (2016) and Tao *et al.* (2017).

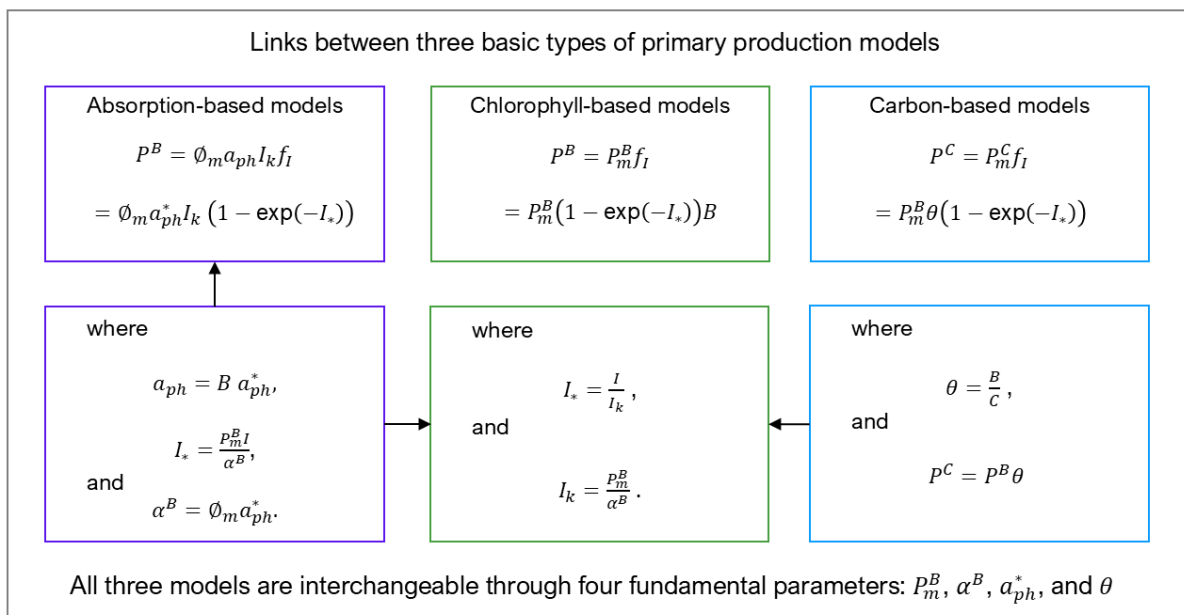
337 Satellite-based model outputs have been compared against *in situ* data, both globally and regionally  
338 (Friedrichs *et al.*, 2009; Saba *et al.*, 2010, Lee *et al.*, 2015). No clear new directions have emerged from these  
339 intercomparisons. A contributing factor to this outcome could be the uncertainty in field measurements of PP and  
340 also to issues related to mismatches between the temporal and spatial resolutions of models and observations.  
341 These inter-comparisons did not examine closely the role of model parameters in the divergence of outputs.  
342 However, the assignment of model parameters remains one of the biggest sources of uncertainty in estimates of  
343 primary production from remote sensing observations (Platt and Sathyendranath, 1993; Sathyendranath and Platt,  
344 2007; Sathyendranath *et al.*, 2009; Kulk *et al.*, 2020, 2021; Brewin *et al.*, 2023).

345 Interestingly, the types of models described above all converge to the same principles and a common set of  
346 parameters (Sathyendranath & Platt, 2007; Figure 4). Chlorophyll-based (or available-light or photosynthesis-  
347 irradiance) models typically use the parameters of the photosynthesis-irradiance curve, normalised to B, the  
348 concentration of chlorophyll-a, i.e., the initial slope ( $\alpha^B$ ) and the assimilation number ( $P_m^B$ ) of the light saturation  
349 curve, and the photoacclimation parameter ( $I_k = P_m^B/\alpha^B$ ) derived from the other two (Platt *et al.*, 1980;  
350 Sathyendranath and Platt, 2007; Figure 4). Absorption-based (which are also called biomass-independent or  
351 inherent-optical-property) models use the realised maximum quantum yield ( $\phi_m$ ) and the absorption coefficient  
352 of phytoplankton ( $a_{ph}$ ) (Kiefer & Mitchell, 1983, Lee *et al.*, 2015). This model can be shown to be equivalent to  
353 the photosynthesis-irradiance models by using the identity  $\phi_m = \alpha^B/a_{ph}$  (Platt *et al.*, 1988; Sathyendranath and  
354 Platt, 2007; Figure 4). The key parameter in carbon-based (or growth) models is the growth rate ( $g$ ), i.e., the rate  
355 of change of carbon per unit time normalised to the initial phytoplankton carbon concentration. The chlorophyll-  
356 to-carbon ratio ( $\theta$ ) can be used to transform growth models to production models and vice versa (Sathyendranath  
357 and Platt, 2007; Sathyendranath *et al.*, 2009). Thus, the different types of satellite-based primary production  
358 models are interchangeable through a common set of parameters: the initial slope ( $\alpha^B$ ) and assimilation number  
359 ( $P_m^B$ ) of the light saturation curve, the mean specific absorption coefficient of phytoplankton ( $a_{ph}^*$ ), and the  
360 chlorophyll-to-carbon ratio ( $\theta$ ) (Sathyendranath and Platt, 2007; Sathyendranath *et al.*, 2009). When the light  
361 incident at the sea surface exceeds a threshold above which light can damage the photosystems, a photo-inhibition

362 term has to be added to the photosynthesis-irradiance equation (Platt *et al.*, 1980). This parameter is often not used  
 363 in satellite-based models; a sensitivity analysis on a photosynthesis-irradiance model (Platt *et al.*, 1990) showed  
 364 that incorporation of realistic values of the photo-inhibition parameter into the model had only small to negligible  
 365 effect on computed water-column primary production, which lends some justification to why this term is often  
 366 ignored. But this is a simplification that can be readily dropped, if new evidence suggests that photo-inhibition  
 367 could be important at large scales.

368 Spectral models of primary production are designed to capture the wavelength-dependent light penetration  
 369 underwater, and wavelength-dependent photosynthesis (Sathyendranath and Platt, 1989). In fully-spectral models,  
 370 the action spectrum of photosynthesis (which describes the wavelength-resolved values of the initial slope  $\alpha^B$ ) is  
 371 coupled to the light available at corresponding wavelengths for photosynthesis (Sathyendranath and Platt, 1989;  
 372 Kyewalyanga *et al.*, 1992), such that the product  $\alpha^B I$  that appears in non-spectral models has to be replaced by  
 373 the wavelength integral  $\int \alpha^B(\lambda) I(\lambda) d\lambda$ , where  $\lambda$  represents the wavelength, and the integral is taken over the  
 374 photosynthetically active range (400-700 nm). The spectral form of the action spectrum closely resembles that of  
 375 the phytoplankton absorption spectrum ( $a_{ph}$ ) (Sathyendranath *et al.*, 1989b; Kyewalyanga *et al.*, 1997). Spectral  
 376 effects are generally considered to be not relevant at saturating light levels. Under light-limiting conditions, if the  
 377 light available is blue-rich, where the action spectrum has a maximum, the coupling between light and  
 378 photosynthesis would be stronger than if the light were green-rich, where the action spectrum typically goes  
 379 through a minimum. We know from previous studies that spectral and non-spectral models may differ from each  
 380 other in a systematic manner (Sathyendranath and Platt, 2007), because non-spectral models are not able to  
 381 account for the covariance (or the lack of it) between spectrally-resolved  $\alpha^B$  and  $a_{ph}$ . To some extent, the impact  
 382 of the spectral effects on water-column primary production could be accommodated into non-spectral models by  
 383 suitably tuning the parameters of non-spectral models (Platt and Sathyendranath, 1991). Typically, therefore, one  
 384 anticipates systematic differences between spectral and non-spectral models of marine primary production, unless  
 385 model parameters are adjusted to compensate for the difference.

386



387

388 **Figure 4.** Phytoplankton absorption-, chlorophyll-a- and carbon-based primary-production models commonly-  
 389 used in satellite-based approaches, and the parameter transformations between them. Notations: Primary  
 390 production ( $P$ ), light-limitation function ( $f_l$ ), as in Table 1, assimilation number of the saturation-light curve, or  
 391 the light saturation parameter ( $P_m^B$ ), initial slope of the light-saturation curve ( $\alpha^B$ ), mean absorption coefficient of  
 392 phytoplankton ( $a_{ph}$ ), chlorophyll-to-carbon ratio ( $\theta$ ), chlorophyll-specific absorption coefficient of  
 393 phytoplankton ( $a_{ph}^*$ ), realised maximum quantum yield of photosynthesis ( $\Phi_m$ ), photoacclimation parameter of  
 394 the light-saturation curve ( $I_k$ ), phytoplankton biomass in chlorophyll-a units ( $B$ ), normalised irradiance ( $I_*$ ),  
 395 irradiance ( $I$ ), phytoplankton carbon biomass ( $C$ ), time ( $t$ ), and growth rate ( $g$ ). One of the ( $f_l$ ) functions from  
 396 Table 1 was selected here for illustrative purposes, but other functions have also been used in the literature. As  
 397 shown below (Figure 7), numerically, most of the ( $f_l$ ) functions are almost identical to each other, unless photo-  
 398 inhibition is introduced. Currently, remote-sensing-based primary-production models do not incorporate the  
 399 photo-inhibition term.

400

### 401 3.2 Ecosystem models

402 Ecosystem models differ greatly in their complexity, ranging from simple, three-component Nutrient-  
 403 Phytoplankton-Zooplankton (NPZ) models (Fasham *et al.*, 1990; Steele and Henderson, 1992; Franks, 2002;  
 404 Gentleman, 2002) to highly complex ones with hundreds of ecosystem components (e.g., Dutkiewicz *et al.*, 2020,  
 405 Fennel *et al.*, 2022). Some models use a single measure for biomass (e.g., carbon), and a single nutrient (usually  
 406 nitrogen) as the model currency, assuming a fixed stoichiometry (relationship between biogeochemically-  
 407 important elements), whereas other models allow for dynamically resolved stoichiometry within  $f_N$ . In this  
 408 section, we focus primarily (but not exclusively) on marine ecosystem models (here used interchangeably with  
 409 “marine biogeochemical models”) that participate in the Climate Model Intercomparison Project (CMIP) (e.g.,  
 410 Laufkotter *et al.*, 2015; Kwiatkowski *et al.*, 2020), as well as regional ecosystem models that are run operationally  
 411 by forecasting centres (e.g., Fennel *et al.*, 2019) for regional climate projections. In these models, PP is usually  
 412 estimated along the lines of Equations 2 and 3, where primary production ( $P$ ) is calculated by multiplying the  
 413 phytoplankton biomass (usually carbon) by its reference growth rate  $g$ , modulated typically by the three  
 414 functions,  $f_T$ ,  $f_N$  and  $f_l$ .

415 There are also many similarities across the ecosystem models that go beyond the functional form of Equation  
 416 2, and a few common approaches can be identified in the equations used to express the functions  $f_T$ ,  $f_N$  and  $f_l$   
 417 (Table 1). For instance,  $f_T$  is typically described through an exponential function (originating from Eppley, 1972;  
 418 e.g., see Laufkotter *et al.*, 2015), that was proposed as an outer envelope of temperature response functions of  
 419 many single phytoplankton species (Eppley, 1972; Norberg, 2004). The response functions of individual  
 420 phytoplankton species could include inhibition temperatures higher than what is optimal for growth of that specific  
 421 species (e.g., Norberg, 2004; Butenschön *et al.*, 2016, Dutkiewicz *et al.*, 2020a), which is linked to Q10, a measure  
 422 of the sensitivity of photosynthesis to temperature. This temperature inhibition of individual phytoplankton  
 423 species is not captured by the exponential function representing the collective response. Furthermore, ecosystem  
 424 models that resolve groups of phytoplankton (e.g., diatoms) do not have temperature inhibition, with the implicit  
 425 assumption that there is a spectrum of diatoms that have temperature optima across the full temperature range (see  
 426 e.g., Anderson *et al.*, 2020). Furthermore, some models do not have explicit PP temperature dependence at all  
 427 (e.g., Daewel and Schrum, 2013). When multiple nutrients are considered, the  $f_N$  function is typically formulated

428 to use Liebig's law of minimum to combine their effects on PP, and is often based either on cell quota of nutrients  
429 within the cells (Droop, 1974), or on the concentrations of the nutrients in the medium (Michaelis and Menten,  
430 1913). In some cases (e.g., Shigemitsu *et al.*, 2012),  $f_N$  is based on the optimal nutrient uptake kinetics (Smith *et*  
431 *al.*, 2009), which allows for parameters in the Michaelis-Menten equation to vary (Table 1). A variety of equations  
432 are currently in use to describe the light-dependence function ( $f_I$ , see Table 1) in ecosystem models, including  
433 those from Platt *et al.* (1980), Steele (1962), and Jassby and Platt (1976), some of which account for the effect of  
434 photo-inhibition at high light, whilst others do not. Furthermore, many of the ecosystem models also include  
435 photoacclimation, either as part of the  $f_I$  function, or as an additional term, mostly following the model of Geider  
436 *et al.* (1997, 1998).

437 Other significant differences across ecosystem photosynthesis models include the number of phytoplankton  
438 functional types and size-classes represented, the number of limiting nutrients included (and the types of equations  
439 selected to represent the role of each nutrient), and the number of wavebands considered in representation of  
440 irradiance (the level to which light is spectrally and directionally resolved, e.g., see Platt and Sathyendranath,  
441 1991; Dutkiewicz *et al.*, 2015; Gregg & Rousseaux, 2016). Practically all ecosystem models include nitrogen  
442 limitation. But iron limitation is also considered important, as is silica limitation, especially in those models that  
443 include diatoms as a phytoplankton class. Phosphate limitation becomes important as well, in particular when  
444 dealing with nitrogen-fixing organisms. Another fundamental difference lies in the representation of the  
445 production and remineralisation of particulate and dissolved organic matter which are included in the models as  
446 explicit or implicit processes, affecting the model parametrisations of GPP, which may or may not include  
447 exudation (e.g., Butenschön *et al.*, 2016; Vichi *et al.*, 2007; Wu *et al.*, 2021).

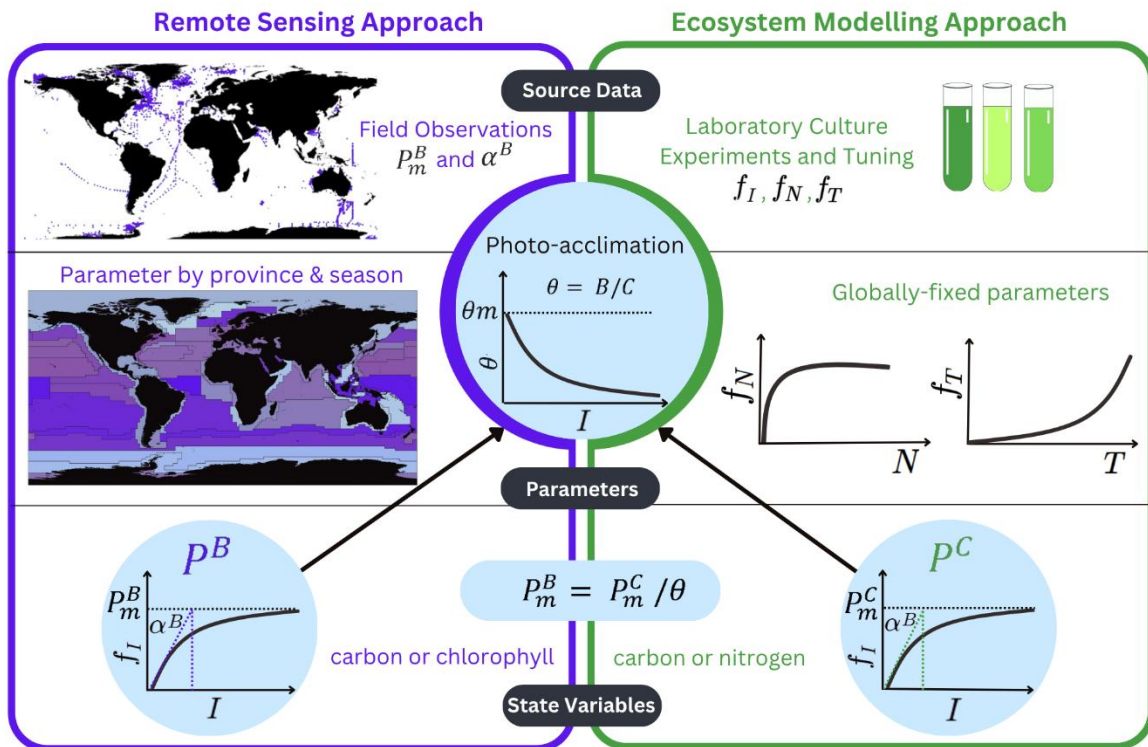
448

### 449 **3.3 Comparison of satellite-based and ecosystem models**

450 Satellite-based and ecosystem models for estimating ocean PP have some similarities, but also key distinctions  
451 (Figure 5; also see IOCCG, 2020). Model parameter assignment provides one clear perspective on a difference  
452 between the two types of models. For example, parameters associated with PP models in the satellite-based  
453 approach of Platt and Sathyendranath (1988), Kulk *et al.* (2020) and Sathyendranath *et al.* (2020) are established  
454 from field observations, whereas ecosystem model parameters are typically estimated using information from  
455 laboratory experiments conducted under controlled conditions, followed by tuning the model towards the available  
456 observations. But here also, the distinction is not clear cut: for example, the carbon-based production model of  
457 Behrenfeld *et al.* (2005) relies on culture measurements to establish growth rate and carbon-to-chlorophyll ratio.  
458 Some satellite-based models that do not have explicit nutrient and temperature dependencies implicitly  
459 incorporate those dependencies in the model parameter values, which are allowed to vary across biogeographical  
460 provinces (Longhurst, 2007) and seasons (e.g., see Figure 6 for photosynthesis-irradiance parameter data  
461 partitioned according to Longhurst provinces), representing different nutrient and temperature environments.  
462 Ecosystem models typically represent the nutrient and temperature limitation explicitly, with different parameters  
463 assigned to each plankton group. Another difference in parameterisation is that many ecosystem models use  
464 maximum carbon or nitrogen-specific production rate under optimal conditions as a model parameter and the  
465 corresponding biomass is then used to scale PP to its absolute value (Figure 5). While carbon-based satellite  
466 algorithms for PP are similar to ecosystem models in this respect, other satellite models rely on bio-optical  
467 properties such as chlorophyll-a concentration or phytoplankton absorption coefficient as the state variable. Some

468 ecosystem models also include a photo-inhibition term, to represent the reduction in photosynthesis under high  
 469 light intensities, whereas satellite-based models typically account only for the saturating response to light without  
 470 including photoinhibition. Photoacclimation is generally addressed by both approaches, with many of them  
 471 relying on variations of the Geider *et al.* (1997, 1998), though there are exceptions (e.g., photoacclimation model  
 472 in Westberry *et al.*, 2008).

473 Finally, the ecosystem models are able to compute depth-resolved PP, as is the case for the satellite-based  
 474 method proposed by Platt and Sathyendranath (1988), whereas some other satellite-based models are designed to  
 475 yield vertically integrated production (e.g., Behrenfeld and Falkowski, 1997).



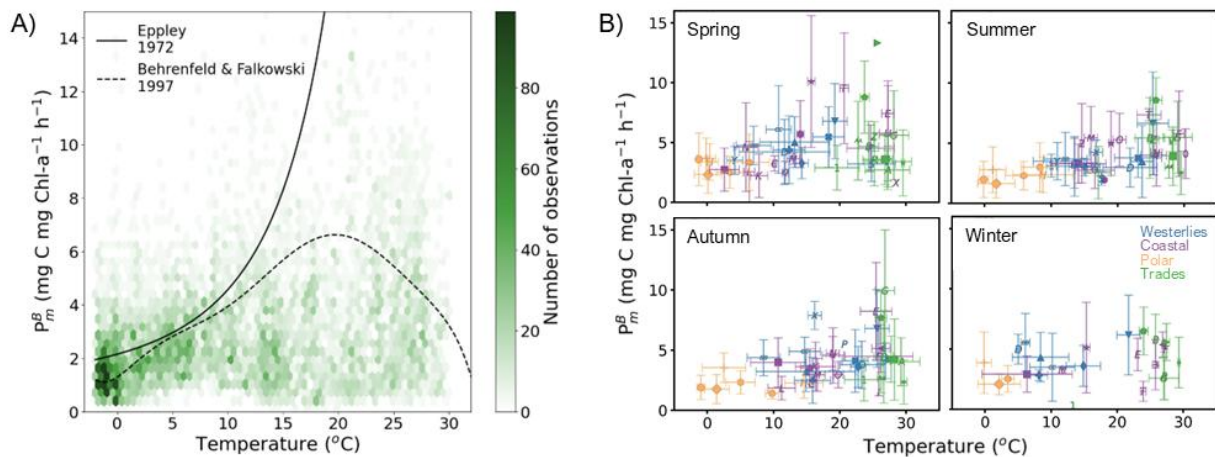
476  
 477 **Figure 5.** Comparison of satellite remote sensing (left) and ecosystem modelling (right) approaches to computing  
 478 marine primary production, and where they interact (light blue) through the photo-acclimation model which is  
 479 essential to enable comparison between the models.  $I$  = Light,  $N$  = Nutrient,  $T$  = Temperature. It should be noted  
 480 that although carbon, or nitrogen, are the most common currency used by the ecosystem models, there are also  
 481 ecosystem models which use chlorophyll-a as the currency.

482  
 483 All satellite-based models are data-rich, in the sense that they are designed to exploit satellite observations,  
 484 typically with global coverage and nominal daily repeat frequency. Some use culture data as auxiliary information;  
 485 others rely on *in situ* field observations. Ecosystem models, on the other hand, tend to be data-sparse; even when  
 486 operated in data assimilation mode, only a fraction of the modelled ecosystem compartments or fluxes are usually  
 487 constrained by assimilation. The constraints imposed by satellite data availability limit the processes and variables  
 488 that can be estimated, whereas ecosystem models tend to be rich in outputs they provide.

489 Platt and Sathyendranath (1997) proposed a hierarchy of PP models (Figure 7). Almost all the types of models  
 490 in this hierarchical classification, other than purely statistical models, are represented in PP models under  
 491 discussion in this paper. With the exception of absorbed-light models that are in use in satellite-based models, but  
 492 not in ecosystem models, the different classes of models are found in both types of models. In this regard, the  
 493 diversity of models within satellite-based or ecosystem-based approaches is no smaller than across those two  
 494 groups of models, though, notably, models that use chlorophyll-a as the state variable are unique to satellite-based  
 495 approaches. (There are sound reasons for the choice of chlorophyll-a concentration as the state variable, in addition  
 496 to the obvious one that it is readily available from ocean-colour data, e.g., Sathyendranath *et al.*, 2023.)

497 When dealing with complex problems such as the one addressed here, it is always an advantage to look at the  
 498 problem from multiple angles. Convergence of solutions add confidence, divergence helps identify sources of  
 499 discrepancy. It is worth emphasising that the relative strengths and weaknesses of ecosystem and satellite-based  
 500 models can be leveraged, once the two types of models become better integrated, as advocated in this paper. We  
 501 provide concrete examples on how the two types of models could be of benefit to each other in the section outlining  
 502 the way forward.

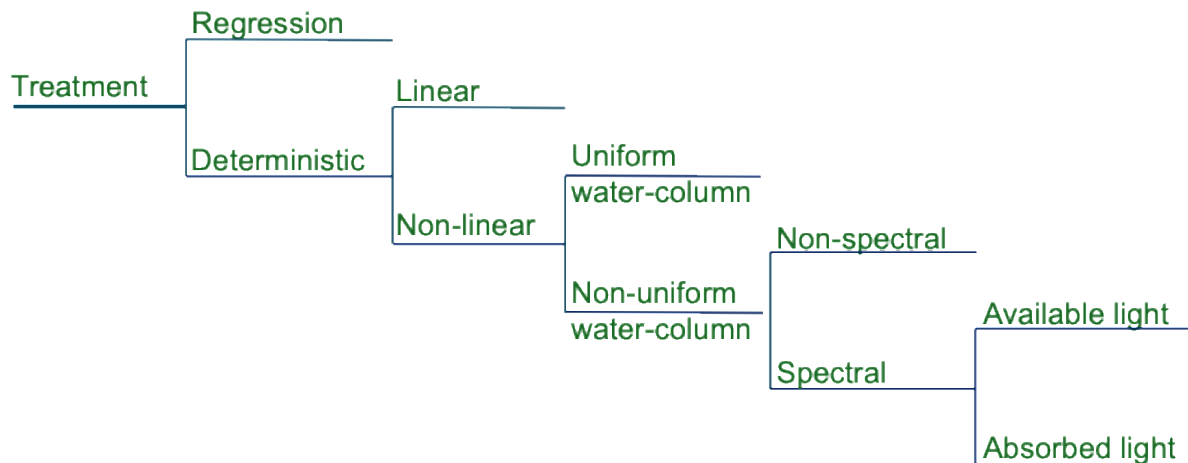
503



504

505 **Figure 6.** Variability in the photosynthesis-irradiance parameter  $P_m^B$  in the ocean. A) Parameter values from a  
 506 global in situ dataset (Bouman *et al.* 2018; Kulk *et al.* 2020) plotted as a function of temperature. Two commonly-  
 507 used temperature-dependent equations (Eppley 1972; Behrenfeld and Falkowski 1997) of this parameter are also  
 508 shown. B) The same data sorted according to ecological provinces of Longhurst (2007) and according to season,  
 509 with colours representing four different oceanic biomes (Longhurst 2007), showing that some structure and pattern  
 510 emerge when the data are organised according to oceanic biomes and to a smaller degree seasons.

## Hierarchy of Primary Production Models



511

512 **Figure 7.** Hierarchy of primary production models. The models get more complete (and more complex), as we go  
 513 from left to right, and from the upper to the lower limb of each branch.

514

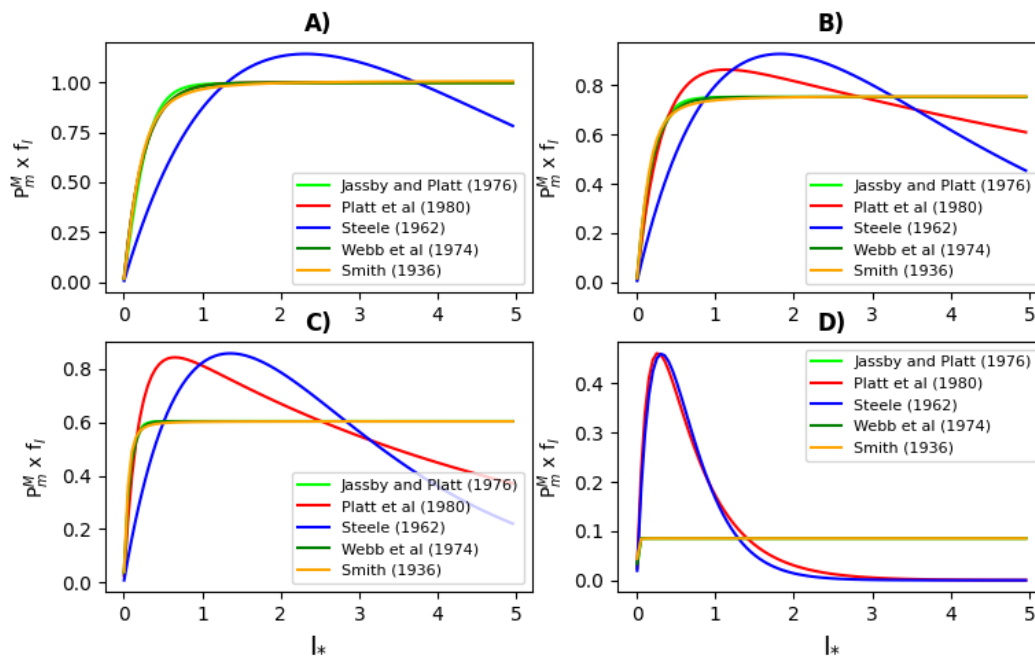
515

#### 516 4. How similar are the different primary production models?

517 Platt and Sathyendranath (1993) showed that we can anticipate systematic biases between satellite-based models  
 518 that are structured differently, and we can theoretically, or numerically predict under what conditions the biases  
 519 relative to each other will manifest themselves. For example, linear and non-linear models are expected to behave  
 520 similarly under low-light levels, but to diverge as light levels increase. The authors also showed that when PP  
 521 models have similar structures, it is possible to reduce all of them to a common, canonical form, revealing that  
 522 apparently-different model types (available light models, absorbed light models, chlorophyll-based or carbon-  
 523 based models) become equivalent when implemented with comparable model parameter values (Platt and  
 524 Sathyendranath, 1993; also see Sathyendranath and Platt, 2007; Sathyendranath *et al.*, 2020). Such comparisons  
 525 also reveal systematic biases between spectral and non-spectral models of PP, arising from spectral effects in both  
 526 underwater light penetration and phytoplankton light utilisation. It has been demonstrated that biases between  
 527 spectral and non-spectral PP models can be minimised by tuning the diffuse attenuation coefficient of  
 528 downwelling irradiance, which determines the rate of change of available light with depth (Platt and  
 529 Sathyendranath, 1991; Kyewalyanga *et al.*, 1992). Similarly, Kovač *et al.* (2016a) demonstrated that a locally  
 530 tuned non-spectral model, with adjusted values of photosynthesis parameters, can outperform a spectral model,  
 531 without locally tuned values of photosynthesis parameters. Such comparisons bring to the fore the importance of  
 532 parameter assessment, assignment, and evaluation to understand model performances, uncertainties and  
 533 divergences, which is at the core of this review.

534 To illustrate the point, let us focus, for example, on the light function ( $f_i$ ), which takes a wide range of forms  
 535 in the literature (see Table 1). Even though the functional forms cannot be analytically transformed into each other  
 536 (they are mathematically different), numerically they could still be very close to each other, in the sense that they  
 537 can all fit the same observations similarly well when the parameters are chosen appropriately (Kovač *et al.*, 2017).  
 538 These different forms split into two classes: one that includes photo-inhibition and the other that does not (Amirian  
 539 *et al.*, 2025). Figure 8 shows that the  $f_i$  models without photo-inhibition (Webb *et al.*, 1974; Jassby and Platt,

540 1976; Smith, 1936) are all practically identical to each other for equivalent parameter values and are therefore  
 541 basically indistinguishable from each other. It should also be noted that the Webb *et al.* (1974) model is a special  
 542 case of the Platt *et al.* (1980) model for the case of zero photo-inhibition. The  $f_i$  model that stands out is the one  
 543 of Steele (1962), which struggles to match the other  $f_i$  models under low-light conditions. However, when photo-  
 544 inhibition is important, the  $f_i$  model of Platt *et al.* (1980) can again nicely match the Steele (1962) model if their  
 545 parameter values are chosen appropriately. What we learn from Figure 8 is that a lot of the diversity in  $f_i$  models  
 546 is only apparent, as the diversity can be eliminated via model parametrisation.



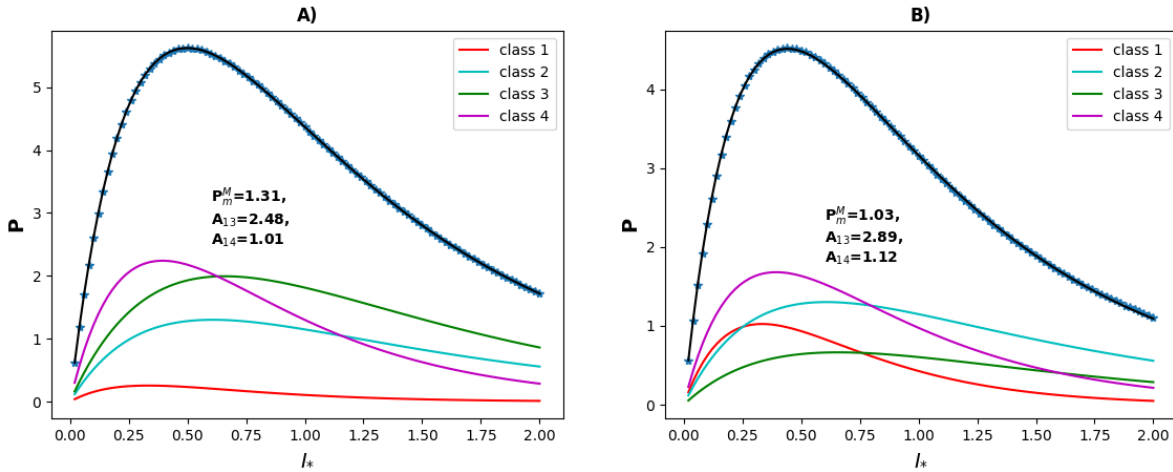
547  
 548 **Figure 8.** Comparing the functional forms of four  $f_i$  models in different regimes. Since only the functional forms  
 549 are compared, the x and y axes do not necessarily represent realistic values of normalized irradiance ( $I_*$ ) or  $f_i$ , and  
 550 the units are arbitrary. The Figure shows the degree to which the five different models can be "tuned" to each  
 551 other through fitting their parameters in a suitable way. The functional forms for the  $f_i$  models presented in this  
 552 figure are introduced in Tab.1, except the model by Webb *et al.* (1974), which is a special case of Platt *et al.*  
 553 (1980) for zero photoinhibition (setting  $A_{14} = 0$ , see Tab.1). Furthermore, what is plotted in this figure is  $f_i$   
 554 multiplied by the scaling factor  $P_m^M$  in Equations 2 and 3. The panels A-D show cases of increasing photoinhibition  
 555 as modelled by the most complex Platt *et al.* (1980) model (A is the lowest, D the highest), with the other models  
 556 tuned to best fit the curve corresponding to Platt *et al.* (1980). We see that the five models essentially split into  
 557 two families, each representing well a limiting case of either no photoinhibition (Jassby and Platt 1976, Webb *et al.*  
 558 *al.* 1974, Smith 1936), or very high photoinhibition (Steele 1962).

559  
 560 In general, PP models are designed to represent limitations to phytoplankton growth (whether from light,  
 561 nutrients or temperature) under different environmental conditions and for different groups of phytoplankton, as  
 562 appropriate. These models have the potential to be generalised to deal with additional external conditions (which  
 563 may not be explicitly included in the model) by incorporating spatially and temporally variable parameter values.  
 564 This flexibility allows models to account for the diversity of phytoplankton and the processes responsible for their  
 565 dynamics, which are not explicitly represented in current models. Representing the full diversity of phytoplankton

566 species is not feasible due to lack of understanding and computational demand, which is why models typically  
567 rely on the use of phytoplankton classes to represent aggregations of multiple species based on shared  
568 characteristics or traits, such as body size, biogeochemical functions, life strategies and behaviours. This approach  
569 captures at best the average or most typical behaviour of each class (e.g., Anderson, 2020; Ratnarajah *et al.*, 2023).  
570 When aggregating species according to their physiological and functional traits and behavioural patterns into a  
571 pre-defined number of modelled classes, fixed values are assigned to model parameters within each aggregated  
572 class. For ecosystem models, many of these parameters have assigned values based on laboratory or mesocosm  
573 experiments (Geider *et al.*, 1998; Schartau *et al.*, 2017; Ratnarajah *et al.*, 2023), often focusing on a small number  
574 of carefully-selected species, far from capturing the full diversity of organisms or their responses and behaviours  
575 that might be expected in the natural environment across large spatio-temporal scales (Geider *et al.*, 1998;  
576 Schartau *et al.*, 2017; Ratnarajah *et al.*, 2023). In contrast, in the natural environment, we can expect parameters  
577 to vary in time and space, reflecting both changes in the governing conditions and in the unresolved functional  
578 diversity in the makeup of modelled planktonic communities (Schartau *et al.*, 2017). Such parameter variability  
579 can be observed in model calibration experiments (e.g., Leeds *et al.*, 2011; Mattern *et al.*, 2012, 2014), including  
580 those using data assimilation to estimate model parameters jointly with the model state (e.g., Pastres *et al.*, 2003;  
581 Tijputra *et al.*, 2007; Roy *et al.*, 2012; Doron *et al.*, 2013; Simon *et al.*, 2015; Gharamti *et al.*, 2017a,b; Skákala  
582 *et al.*, 2024).

583 A simple illustration of how parameter variability emerges from aggregating species into classes is provided  
584 in Figure 9. Although models differ from each other in the number of phytoplankton classes they resolve, for each  
585 phytoplankton class they typically use the same functional form to describe photosynthesis, with total  
586 phytoplankton PP corresponding to the sum of contributions across all classes. Figure 9 demonstrates that models  
587 with different numbers of classes become equivalent in their description of total PP, provided that the parameters  
588 in models with fewer classes are allowed to vary with space and time. In such a way, spatio-temporal parameter  
589 variations could effectively capture the influence of unresolved diversity in phytoplankton community structure,  
590 in models with only a few phytoplankton classes. The spatio-temporal model parameter variations would then be  
591 a consequence of the models' inability to sufficiently resolve phytoplankton species, which also means that such  
592 parameter variability would be expected to be especially relevant for the simpler models (e.g., ecosystem models  
593 typically used in ESMs). The more complex models currently in use (e.g., DARWIN; see Ward *et al.*, 2012;  
594 Dutkiewicz *et al.*, 2020a) would have less reason to adopt spatio-temporally variable parameters; but these models  
595 are typically too computationally expensive to be run as part of ESMs in long-term ensemble-based climate  
596 projections. Furthermore, even as complex as they are, they still represent only a fraction of the real-world  
597 diversity. On the other hand, as the models get more complex by incorporating more ecosystem compartments,  
598 the challenge shifts to calibrating each of the large numbers of parameters to adequately capture the functions of  
599 each of the model components.

600



601

602 **Figure 9.** A simple illustration of how unresolved phytoplankton community structure can lead to parameter  
 603 variability. In both panels, we plot PP expressed as  $P = P_m^M \cdot f_I(I_*)$ .  $M$  with functional form  $f_I$  corresponding to  
 604 the Platt *et al.* (1980) model (see Tab.1). As in Fig. 8, ranges of scaled irradiance,  $I_*$ , and PP values are arbitrary.  
 605 Four phytoplankton classes are plotted, each with different  $P_m^M, A_{13}, A_{14}$  parameters. The dark blue dots are  
 606 obtained by summing up the PP across the four classes (this corresponds to PP of total phytoplankton) and the  
 607 dark blue line is the fit of the points with the same functional form used for the four phytoplankton classes  
 608 assuming the total phytoplankton concentration is the sum of the concentrations of the four classes. The two panels  
 609 show two situations where the same total phytoplankton concentration is distributed into classes in different ways  
 610 (the phytoplankton community structure changes). We can see that if we did not resolve the four classes, we could  
 611 still use the Platt *et al.* (1980) model (including photoinhibition) for the total phytoplankton, but the parameters  
 612  $P_m^M, A_{13}$ , and  $A_{14}$  would vary depending on the (unresolved) variations in the phytoplankton community structure.  
 613

## 614 5. A way forward

615 Together, these considerations suggest that investigating parameter assignment and parameter variability may be  
 616 an important route to understand and potentially reduce many of the apparent differences between marine PP  
 617 models, and hence in the estimated magnitudes of production. Investigation into the role of parameters should be  
 618 followed by a consistent calibration against observational data. To estimate spatially and temporally varying  
 619 parameters in ecosystem models, data assimilation can provide a natural tool for model calibration (e.g., Tjiputra  
 620 *et al.*, 2007; Singh *et al.*, 2025). However, introducing spatio-temporally variable (or too many constant)  
 621 parameters comes with its own challenges. For example, allowing the (often many) model parameters to vary  
 622 substantially increases model flexibility, but at the risk of overfitting to observations, particularly if the number  
 623 of model parameters is large or observational data are insufficient. Overfitting may reduce the model ability in  
 624 predicting new phenomena, including future climate-driven changes. It is therefore essential that the introduction  
 625 of variable parameters takes into account such risks and ensures that reasonable assumptions are made to simplify  
 626 the parameter calibration task. These assumptions would ensure that model calibration is sufficiently constrained,  
 627 so that there are sufficient observations per each calibrated model parameter value. For example, only a carefully  
 628 selected subset of parameters may be calibrated, based on their relevance for PP (established, for example, through  
 629 sensitivity analysis, e.g., Ciavatta *et al.*, 2025) and lack of correlations with other model parameters.

630 A key consideration when exploring variable parameters is the spatial and temporal scales at which they  
631 might vary. For example, it would be important to establish whether seasonal, climatological variability in  
632 parameters would be sufficient to capture observed patterns, implying that variability at shorter (sub-seasonal)  
633 and longer (inter-annual) time scales could be negligible. If so, this would relax the requirement on the volumes  
634 of observational data needed for the calibration, and also on the need to continually update parameter values from  
635 day to day or year to year. Hypotheses about temporal variability scales for model parameters can be tested using  
636 long time-series of measurements at specific stations, such as the Bermuda Atlantic Time-series Study and the  
637 Hawaii Ocean Time-series, both of which present seasonal cycles in photosynthesis parameters (Kovač *et al.*,  
638 2016b; Kovač *et al.*, 2018). Another key question is whether parameters vary over fine spatial scales or maintain  
639 coherence over large scales such as within ocean biomes or Longhurst provinces (Longhurst, 2007). Preliminary  
640 evidence suggests that, at least for the global-scale applications, ecological provinces according to Longhurst  
641 might provide an appropriate template for mapping parameters (see Figure 6B), and that monthly or seasonal time  
642 scales might be appropriate for modelling variability in photosynthesis-irradiance parameters (Britten *et al.*, 2025).  
643 If province-based approaches emerge as viable candidates, it would be desirable to avoid sharp discontinuities in  
644 parameter values at province boundaries, which might require incorporation of smoothing methods to make inter-  
645 province changes seamless. Moreover, it is essential that model parameter calibration does not compensate for  
646 unrelated spatio-temporally varying model biases, such as those arising from external forcings or other ecosystem  
647 model constraints (e.g., boundary conditions). For example, given the importance of underlying physical  
648 processes, caution should be applied when calibrating parameters in ecosystem models to avoid models better  
649 reproducing the observed PP, but for the wrong reasons. Singh *et al.* (2025) illustrate that ecosystem parameters  
650 in global ocean biogeochemical models are likely calibrated to compensate for biases in their physics (see also  
651 Loptien and Dietze, 2019). To avoid mixing different sources of ecosystem model errors, parameters should be  
652 ideally estimated jointly with the model state, e.g., using joint parameter-state data assimilation techniques  
653 (Schartau *et al.*, 2017). Finally, existing knowledge of acceptable ranges of parameter values needs to be  
654 incorporated into the calibration process to prevent parameters from acquiring unrealistic values.

655 Since parameter spatio-temporal variability results from poorly resolved species types or ecosystem  
656 processes, interesting insights into its scale and patterns can be also obtained by comparing models of different  
657 complexity. For example, high-complexity ecosystem models (such as the DARWIN ecosystem model) could be  
658 used in some cases to deduce the degree of parameter variability of simpler ecosystem models or help inform  
659 spatio-temporally varying parameter calibration of those models (always keeping in mind that inter-model  
660 consistency does not automatically imply model quality). Comparison studies across models of different  
661 complexity would be desirable in this case (for some examples see Friedrichs *et al.*, 2007; Xiao and Friedrichs,  
662 2014). Similarly, emergent properties of ecosystem models can be leveraged to provide specific information for  
663 satellite-based models, such as vertical and class-distribution of phytoplankton (e.g., Stock, 2019), or information  
664 about nutrient distributions. Such inter-calibrations of models against each other could potentially improve  
665 satellite PP products and conversely make the satellite PP data more useful for ecosystem model development.  
666 However, one has to be cautious here: model-model intercomparisons and tuning would help models look more  
667 like each other, but independent information would be needed to ensure that the simulations are also getting closer  
668 to key features in the real world that the models are designed to reproduce.

669 Even after successfully overcoming the challenges associated with spatio-temporal parameter calibration,

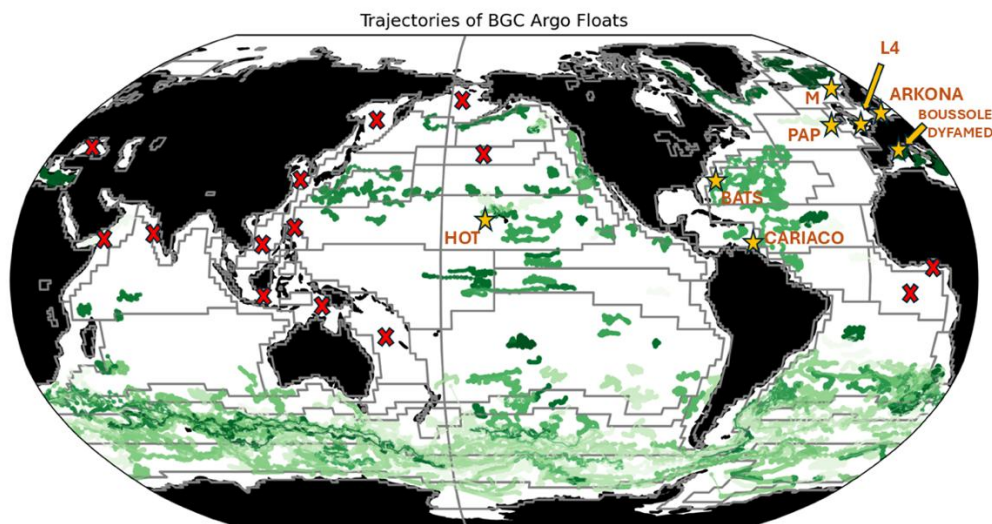
670 significant PP uncertainty is likely to remain in both historical estimates and future projections. For satellite-based  
671 models, residual uncertainties could be associated with inherent observational biases, e.g., gaps in data due to  
672 cloud cover or adverse viewing geometry, or inaccuracies in satellite products associated with bio-optical  
673 conditions in water, or biases inherited from calibration against *in situ* PP observations with their own inherent  
674 uncertainties. For ecosystem models, additional sources of uncertainty include the forcing data and the physical  
675 model driving biogeochemical processes, e.g., its vertical and horizontal resolution, and its ability to represent  
676 currents and mixing responsible for nutrient supply and export of organic material. For example, differences in  
677 how models treat external forcing, such as micro- and macronutrient depositions from the atmosphere, could still  
678 contribute to the growth of uncertainties as models become more complex. Furthermore, the spread in the  
679 underlying environmental changes such as warming, stratification, changes in irradiation, and ocean circulation  
680 among others, contributes significantly to uncertainties in the PP projection.

681 Further constraints are inherent to ecosystem models themselves. Traditionally, plankton are divided into  
682 phototrophic phytoplankton and phagotrophic zooplankton. However, recent research emphasises ubiquitous  
683 presence of mixotrophy in the global ocean (Mitra *et al.*, 2023), which not only differs in its physiology and  
684 ecological role, but also in its complex interactions with other types of plankton (Flynn and Mitra, 2023). Despite  
685 certain commonality in their approach to modelling PP, as discussed above, models differ significantly in their  
686 approaches to representing various biogeochemical processes such as grazing and associated fluxes, deposition of  
687 organic matter and its remineralisation. For many of those processes (e.g., zooplankton grazing), lack of data, and  
688 variability and high uncertainty of available data, are major issues. Focusing on biological ocean carbon storage,  
689 Henson *et al.* (2024) identified key areas where improved understanding of processes is required to support future  
690 modelling efforts. For PP, the processes that were ranked highest were: resource limitation for growth, nitrogen  
691 fixation, zooplankton processes and phytoplankton loss processes. Current ecosystem models differ considerably  
692 in their formulation and parameterisation of these processes, contributing to uncertainties in model outcomes.  
693 Moreover, nitrogen-fixation is often not included in these models. Even when these key processes are included,  
694 spatial parameter estimation through assimilating observed state variables (such as water column nutrients and  
695 oxygen) in ocean biogeochemical models does not necessarily lead to an improved estimate of PP, suggesting that  
696 current ecosystem model parameterisations may still be oversimplified compared with the real world (Singh *et al.*,  
697 2025).

698 The time is right to address the problem of parameter estimation in PP models, both for ecosystem models  
699 and satellite-based models. Novel and rapidly expanding observations such as BGC Argo profiles, other types of  
700 autonomous data collected by in-water vehicles and also large marine mammals (Chai *et al.*, 2020; Claustre *et al.*,  
701 2020) have been providing large volumes of biological and bio-optical data that complements *in situ* data from  
702 long time series stations, and could be harnessed for this purpose (Figure 10). Complementary observations from  
703 satellite remote sensing, now available over multiple decades and merged into climate-quality, consistent data  
704 streams (e.g., Sathyendranath *et al.*, 2019), is another rich data source, along with novel satellite products from  
705 emerging capabilities such as geostationary, lidar, cubesat and hyperspectral data. When these are combined with  
706 more traditional *in situ* platforms, including long-term gridded climatology from sources such as World Ocean  
707 Atlas (WOA, e.g., Garcia *et al.*), and potentially complemented by the intercomparison of models with different  
708 complexity, there is in several cases already enough data to support a suitably-constrained spatio-temporally  
709 varying parameter calibration. This opportunity is further enhanced by new advances in artificial intelligence (AI)

710 and machine learning (ML), giving us an historically unprecedented capability to exploit large and growing  
711 datasets to address long-standing questions about marine PP. AI can be used in a variety of different ways, either  
712 as a direct prediction approach to optimise model parameterisation and also to emulate models, allowing it to  
713 explore a range of model behaviours at reduced computational cost for parameter sensitivity analyses and model  
714 calibration (e.g., Mattern *et al.*, 2012; Schartau *et al.*, 2017). Furthermore, recent statistical approaches unique to  
715 the ML field enable insights into what the ML model has learned, for example, using Explainable AI, or physically  
716 constrained machine learning.

717 However, crucial to this endeavour would be a clear focus on data quality, and on data validation, following  
718 community-wide accepted protocols and reliable uncertainty characterisation. Moreover, some regions, such as  
719 sea-ice margins, coastal margins, and high latitudes in winter, which are often regions experiencing long-term  
720 rapid changes and include some of the most productive areas of the global ocean, also tend to be regions that are  
721 difficult to observe, and hence suffer from sparse data coverage. More observations are needed in such locations  
722 to understand the behaviour of model parameters in such regions, including their future changes. Even if  
723 constrained spatio-temporally varying calibration is possible in these regions with the available datasets, the  
724 importance of further investing in data quantity and quality cannot be overemphasised.



725  
726 **Figure 10.** The global in situ data available for model calibration. The boundaries show ecological provinces  
727 according to Longhurst (2007). BGC-Argo float trajectories are shown in shades of green, providing sufficiently  
728 long time-series (since 2008) for calibration. Orange stars mark in situ time series stations with sufficiently long  
729 time-series records that can also be used for model calibration. The red crosses mark provinces without sufficient  
730 BGC-Argo data or in situ stations, where the models will need to rely solely on satellite records and compilations  
731 of in situ observations, such as the World Ocean Atlas.

732

## 733 6. Conclusions

734 We have argued that, given the growing abundance of observations from diverse platforms, such as satellites and  
735 BGC-Argo, combined with rapidly advancing capabilities in ensemble data assimilation techniques and artificial  
736 intelligence, the time has now come to address explicitly the importance of parameter assignment in primary  
737 production models, and in exploring the spatial and temporal variability in the parameters. We have theoretically  
738 justified why such parameter variability is to be expected both in the satellite-based models (where some models

739 already employ variable parameters albeit in a simple fashion) and ecosystem models (where assignment of  
740 variable parameters is still quite rare), at least in models are of high complexity. In the case of primary production,  
741 the number of phytoplankton classes that are included in the model is a key differentiator of the model complexity.  
742 Relatively simpler models, such as the ecosystem models used as part of ESMs in climate projections, have limited  
743 capability to resolve phytoplankton communities. For such models, spatio-temporally varying parameters could  
744 provide a means to account for the unresolved phytoplankton variability and processes.

745 Spatio-temporally variable parameter calibration can shed light on the sources of differences between low  
746 or medium complexity ecosystem models typically used in ESMs and satellite-based primary-production models.  
747 Since variable parameters can capture, in a simple manner, processes or conditions that are not explicitly included  
748 in a model, analysing the drivers of parameter variability could help identify how best to overcome current model  
749 drawbacks. Furthermore, providing those models with spatio-temporally varying parameters could remove many  
750 apparent differences between models, both potentially reducing the spatial and temporal biases in model parameter  
751 calibration and enabling the simpler ecosystem models to better represent the effects of unresolved processes or  
752 phytoplankton classes. It would also create opportunities for improved intercomparison across models of different  
753 complexity, including the ability to understand more about unresolved variability in simpler models by comparing  
754 them with the higher-complexity models. One could argue that the spatio-temporally varying parametrisation  
755 could help reduce the existing high uncertainty both in historical estimates and future projections of marine PP,  
756 provided that independent information is used to avoid all models converging towards a systematically biased  
757 outcome. Due to the importance of primary production for climate research, improving its prediction can have a  
758 major impact on both climate mitigation and adaptation planning.

759 In the context of our climate, we need to understand how marine ecosystems in general, and phytoplankton  
760 in particular, respond to change. Three types of changes need investigation: changes in (i) phytoplankton biomass  
761 (whether they be measured as chlorophyll-a, carbon or nitrogen concentration, or all of them); (ii) the rates of  
762 biological processes, with marine primary production being a key process in the global carbon cycle; and (iii)  
763 community structure. All these objectives are intimately linked to parameter variability, with the third one in  
764 particular calling for resolution of parameter variability at the level of major components of the phytoplankton  
765 community.

766 For many decades, we have relied on comparisons and analyses of (both satellite and ecosystem) model  
767 outputs with each other, and with *in situ* data, for insights into model performance, and for identifying the way  
768 forward. It is now time to shift the emphasis toward understanding the behaviour of model parameters, across  
769 models, across multiple phytoplankton types, and across multiple spatial and temporal scales. This focus has the  
770 potential to reduce uncertainties, unify divergent model results, and provide a stronger foundation for predicting  
771 marine primary production under changing climatic conditions.

772 **Code/data availability:** No new data, or code published in this paper.

773 **Author contributions:** JS organized the writing of the manuscript with substantial input by SS, and all the  
774 authors contributed ideas, text and Figures.

775 **Competing interests:** The authors declare that they have no conflict of interest.

776

777 **Acknowledgments:** This work was funded by the European Space Agency (ESA) project Climate and Marine  
778 Production (CAMP). JS, YA, GL, DB also acknowledge UK National Capability funding Atlantic Climate and  
779 Environment Strategic Science (Atlantis). RJWB was supported by a UK Research and Innovation Future Leader  
780 Fellowship (MR/V022792/1). SD acknowledges the Simons Collaboration on Computational Biogeochemical  
781 Modelling of Marine Ecosystem (CBIOMES) (549931). BJ was supported by NASA (80NSSC21K0563,  
782 Lagrangian analyses of ocean color and 80LARC21DA002 – GLIMR). ZK and MBK were supported in part by  
783 the Croatian Science Foundation under the project number IP-2022-10-8859. FM thanks NERC for its support  
784 (NE/X001261/1), RS is funded by the UKRI-NERC TerraFIRMA (NE/W004895/1) project, OU was supported  
785 by a Royal Society Wolfson Visiting Fellowship (grant RSWVF\R3\223016), JT acknowledges the European  
786 Union's Horizon 2020 (grant no. 817578), the European Union under grant agreement no. 101083922 (OceanICU)  
787 and UK Research and Innovation (UKRI) under the UK government's Horizon Europe funding guarantee (grant  
788 numbers 10054454, 10063673, 10064020, 10059241, 10079684, 10059012, 10048179).

789

## 790 **References**

791 Amirian, M. M., Finkel, Z. V., Devred, E., Irwin, A. J. (accepted). Parametrization of Photoinhibition for  
792 Phytoplankton. *Communications Earth and Environment*.

793

794 Anderson, S.I., A.D. Barton, S. Clayton, S. Dutkiewicz, and T. Rynearson, 2021. Marine phytoplankton functional  
795 types exhibit diverse responses to thermal change. *Nature Communications*, doi:10.1038/s41467-021-26651

796

797 Antoine D, Andre J-M, Morel A (1996). Oceanic primary production: 2. Estimation at global scale from satellite  
798 (Coastal Zone Color Scanner) chlorophyll. *Global Biogeochemical Cycles*, 10:57-69.  
799 <https://doi.org/10.1029/95GB02832>

800

801 Arteaga, L.A., Behrenfeld, M.J., Boss, E. and Westberry, T.K., 2022. Vertical structure in phytoplankton growth  
802 and productivity inferred from biogeochemical-Argo floats and the carbon-based productivity model. *Global*  
803 *Biogeochemical Cycles*, 36(8), p.e2022GB007389.

804

805 Behrenfeld, M.J. and Falkowski, P.G. (1997) Photosynthetic Rates Derived from Satellite-based Chlorophyll  
806 Concentration. *Limnology and Oceanography*, 42, 1-20. <https://doi.org/10.4319/lo.1997.42.1.0001>

807

808 Behrenfeld MJ, Boss E, Siegel D, and Shea DM (2005) Carbon-based ocean productivity and phytoplankton  
809 physiology from space. *Global Biogeochemical Cycles* 19. <https://doi.org/10.1029/2004GB002299>.

810

811 Bergas-Masso, E., Hamilton, D.S., Myriokefalitakis, S., Rathod, S., Gonçalves Ageitos, M. and Pérez García-  
812 Pando, C., 2025. Future climate-driven fires may boost ocean productivity in the iron-limited North  
813 Atlantic. *Nature Climate Change*, pp.1-9.

814

815 Blackford, J. C., Allen, J. I., and Gilbert, F. J.: Ecosystem dynamics at six contrasting sites: a generic modelling  
816 study, *J. Marine Syst.*, 52, 191–215, 2004

817

818 Bopp, L., Resplandy, L., Orr, J. C., Doney, S. C., Dunne, J. P., Gehlen, M., Halloran, P., Heinze, C., Ilyina, T.,  
819 Séférian, R., Tjiputra, J., and Vichi, M.: Multiple stressors of ocean ecosystems in the 21st century: projections  
820 with CMIP5 models, *Biogeosciences*, 10, 6225–6245, <https://doi.org/10.5194/bg-10-6225-2013>, 2013.

821

822 Bopp, L., Aumont, O., Kwiatkowski, L., Clerc, C., Dupont, L., Ethé, C., Gorgues, T., Sférian, R., and Tagliabue,  
823 A.: Diazotrophy as a key driver of the response of marine net primary productivity to climate change,  
824 *Biogeosciences*, 19, 4267–4285, <https://doi.org/10.5194/bg-19-4267-2022>, 2022

825

826 Bouman, H.A., Platt, T., Doblin, M., Figueiras, M.G., Gudmundsson, K., Gudfinnsson, H.G., Huang, B.,  
827 Hickman, A., Hiscock, M., Jackson, T., Lutz, V.A., Mélin, F., Rey, F., Pepin, P., Segura, V., Tilstone, G.H., van  
828 Dongen-Vogels, V., Sathyendranath, S. (2018) Photosynthesis–irradiance parameters of marine phytoplankton:  
829 synthesis of a global data set. *Earth Syst. Sci. Data*, 10: 251–266. <https://doi.org/10.5194/essd-10-251-2018>

830

831 RJW Brewin, GH Tilstone, T Jackson, T Cain, PI Miller (2017) Modelling size-fractionated primary production  
832 in the Atlantic Ocean from remote sensing. *Progress in Oceanography*. 158: 130-149, ISSN 0079-6611,  
833 <https://doi.org/10.1016/j.pocean.2017.02.002>.

834

835 Brewin, R.J., Sathyendranath, S., Kulk, G., Rio, M.H., Concha, J.A., Bell, T.G., Bracher, A., Fichot, C., Frölicher,  
836 T.L., Galí, M. and Hansell, D.A., 2023. Ocean carbon from space: Current status and priorities for the next  
837 decade. *Earth-science reviews*, 240, p.104386.

838

839 Butenschön, M., Clark, J., Aldridge, J.N., Allen, J.I., Artioli, Y., Blackford, J., Bruggeman, J., Cazenave, P.,  
840 Ciavatta, S., Kay, S., Lessin, G. *et al.*, 2016. ERSEM 15.06: a generic model for marine biogeochemistry and the  
841 ecosystem dynamics of the lower trophic levels. *Geoscientific Model Development*, 9(4), pp.1293-1339.

842

843 Carr, M.E., Friedrichs, M.A., Schmeltz, M., Aita, M.N., Antoine, D., Arrigo, K.R., Asanuma, I., Aumont, O.,  
844 Barber, R., Behrenfeld, M. and Bidigare, R., 2006. A comparison of global estimates of marine primary production  
845 from ocean color. *Deep Sea Research Part II: Topical Studies in Oceanography*, 53(5-7), pp.741-770.

846

847 Chai, F., Johnson, K.S., Claustre, H., Xing, X., Wang, Y., Boss, E., Riser, S., Fennel, K., Schofield, O. and Sutton,  
848 A., 2020. Monitoring ocean biogeochemistry with autonomous platforms. *Nature Reviews Earth &*  
849 *Environment*, 1(6), pp.315-326.

850

851 Ciavatta, S., Lazzari, P., Álvarez, E., Bertino, L., Bolding, K., Bruggeman, J., Capet, A., Cossarini, G., Daryabor,  
852 F., Nerger, L., Popov, M. *et al.*, 2025. Control of simulated ocean ecosystem indicators by biogeochemical  
853 observations. *Progress in Oceanography*, 231, p.103384.

854

855 Claustre, H, and Johnson, KS, and Takeshita, Y (2020) Observing the Global Ocean with Biogeochemical-Argo.  
856 *Annual Review of Marine Science*,12: 23-48. <https://doi.org/10.1146/annurev-marine-010419-010956>

857

858 Daewel, U. and Schrum, C., 2013. Simulating long-term dynamics of the coupled North Sea and Baltic Sea  
859 ecosystem with ECOSMO II: Model description and validation. *Journal of Marine Systems*, 119, pp.30-49.

860

861 Dai, R., Wen, Z., Hong, H., Browning, T.J., Hu, X., Chen, Z., Liu, X., Dai, M., Morel, F.M. and Shi, D., 2025.  
862 Eukaryotic phytoplankton drive a decrease in primary production in response to elevated CO<sub>2</sub> in the tropical and  
863 subtropical oceans. *Proceedings of the National Academy of Sciences*, 122(11), p.e2423680122.  
864

865 Doléac, S., Lévy, M., El Hourany, R., and Bopp, L.: Toward more robust net primary production projections in  
866 the North Atlantic Ocean, *Biogeosciences*, 22, 841–862, <https://doi.org/10.5194/bg-22-841-2025>, 2025.  
867

868 Doney, S., Bopp, L., Long, M (2014) Historical and Future Trends in Ocean Climate and Biogeochemistry.  
869 *Oceanography*. 27 (1), pp.108-119. [ff10.5670/oceanog.2014.14ff](https://doi.org/10.5670/oceanog.2014.14ff). [ffhal-03211060f](https://doi.org/10.1002/ffhal-03211060f)  
870

871 Doron M, Brasseur P, Brankart JM, Losa SN, Melet A. Stochastic estimation of biogeochemical parameters from  
872 Globcolour ocean colour satellite data in a North Atlantic 3D ocean coupled physical–biogeochemical model.  
873 *Journal of Marine Systems*. 2013 May 1;117:81-95.  
874

875 Droop, M. R.: The nutrient status of alga cells in continuous culture, *J. Mar. Biol. Assoc. UK*, 54, 825–855,  
876 [doi:10.1016/0924-7963\(94\)00031-6](https://doi.org/10.1016/0924-7963(94)00031-6), 1974  
877

878 Dutkiewicz, S., J.R. Scott, and M.J. Follows, 2013, Winners and Losers: Ecological and Biogeochemical Changes  
879 in a Warming Ocean. *Global Biogeochemical Cycles*, 27, 463-477, [doi: 10.1002/gbc.20042](https://doi.org/10.1002/gbc.20042)  
880

881 Dutkiewicz, S., Hickman, A.E., Jahn, O., Gregg, W.W., Mouw, C.B. and Follows, M.J., 2015. Capturing optically  
882 important constituents and properties in a marine biogeochemical and ecosystem model. *Biogeosciences*, 12(14),  
883 pp.4447-4481.  
884

885 Dutkiewicz, S., Cermeno, P., Jahn, O., Follows, M.J., Hickman, A.E., Taniguchi, D.A. and Ward, B.A., 2020.  
886 Dimensions of marine phytoplankton diversity. *Biogeosciences*, 17(3), pp.609-634.  
887

888 Eppley, R., 1972. Temperature and phytoplankton growth in the sea. *Fishery bulletin*, 70(4), p.1063  
889

890 Fasham, MJR, Ducklow, HW, McKelvie, SM (1990) A nitrogen-based model of plankton dynamics in the oceanic  
891 mixed layer. *Journal of Marine Research*, 48: 591-639.  
892

893 Fennel, K., Gehlen, M., Brasseur, P., Brown, C.W., Ciavatta, S., Cossarini, G., Crise, A., Edwards, C.A., Ford,  
894 D., Friedrichs, M.A. and Gregoire, M., 2019. Advancing marine biogeochemical and ecosystem reanalyses and  
895 forecasts as tools for monitoring and managing ecosystem health. *Frontiers in Marine Science*, 6, p.89.  
896

897 Fennel, K., Mattern, J.P., Doney, S.C., Bopp, L., Moore, A.M., Wang, B. and Yu, L., 2022. Ocean biogeochemical  
898 modelling. *Nature Reviews Methods Primers*, 2(1), p.76.  
899

900 Field, CB, Behrenfeld, MJ, Randerson, JT, Falkowski, P (1998) Primary Production of the Biosphere: Integrating  
901 terrestrial and oceanic Components. *Science* 281, 237-240. DOI: 10.1126/science.281.5374.237  
902

903 Flynn, K.J. and Mitra, A., 2023. Feeding in mixoplankton enhances phototrophy increasing bloom-induced pH  
904 changes with ocean acidification. *Journal of Plankton Research*, 45(4), pp.636-651.  
905

906 Franks, P.J.S., 2002. NPZ models of plankton dynamics: their construction, coupling to physics, and application.  
907 *J. Oceanogr.* 58, 379–387. DOI: 10.1023/a:1015874028196.  
908

909 Friedlingstein, P., O'Sullivan, M., Jones, M. W., Andrew, R. M., Bakker, D. C. E., Hauck, J., Landschützer, P.,  
910 Le Quéré, C., Lujckx, I. T., Peters, G. P., Peters, W., Pongratz, J., Schwingshackl, C., Sitch, S., Canadell, J. G.,  
911 Ciais, P., Jackson, R. B., Alin, S. R., Anthoni, P., Barbero, L., Bates, N. R., Becker, M., Bellouin, N., Decharme,  
912 B., Bopp, L., Brasika, I. B. M., Cadule, P., Chamberlain, M. A., Chandra, N., Chau, T.-T.-T., Chevallier, F., Chini,  
913 L. P., Cronin, M., Dou, X., Enyo, K., Evans, W., Falk, S., Feely, R. A., Feng, L., Ford, D. J., Gasser, T., Ghattas,  
914 J., Gkritzalis, T., Grassi, G., Gregor, L., Gruber, N., Gürses, Ö., Harris, I., Hefner, M., Heinke, J., Houghton, R.  
915 A., Hurtt, G. C., Iida, Y., Ilyina, T., Jacobson, A. R., Jain, A., Jarníková, T., Jersild, A., Jiang, F., Jin, Z., Joos, F.,  
916 Kato, E., Keeling, R. F., Kennedy, D., Klein Goldewijk, K., Knauer, J., Korsbakken, J. I., Körtzinger, A., Lan,  
917 X., Lefèvre, N., Li, H., Liu, J., Liu, Z., Ma, L., Marland, G., Mayot, N., McGuire, P. C., McKinley, G. A., Meyer,  
918 G., Morgan, E. J., Munro, D. R., Nakaoka, S.-I., Niwa, Y., O'Brien, K. M., Olsen, A., Omar, A. M., Ono, T.,  
919 Paulsen, M., Pierrot, D., Pocock, K., Poulter, B., Powis, C. M., Rehder, G., Resplandy, L., Robertson, E.,  
920 Rödenbeck, C., Rosan, T. M., Schwinger, J., Séférian, R., Smallman, T. L., Smith, S. M., Sospedra-Alfonso, R.,  
921 Sun, Q., Sutton, A. J., Sweeney, C., Takao, S., Tans, P. P., Tian, H., Tilbrook, B., Tsujino, H., Tubiello, F., van  
922 der Werf, G. R., van Ooijen, E., Wanninkhof, R., Watanabe, M., Wimart-Rousseau, C., Yang, D., Yang, X., Yuan,  
923 W., Yue, X., Zaehle, S., Zeng, J., and Zheng, B.: Global Carbon Budget 2023, *Earth Syst. Sci. Data*, 15, 5301–  
924 5369, <https://doi.org/10.5194/essd-15-5301-2023>, 2023.  
925

926 Friedlingstein, P., O'sullivan, M., Jones, M.W., Andrew, R.M., Hauck, J., Landschützer, P., Le Quéré, C., Li, H.,  
927 Lujckx, I.T., Olsen, A. and Peters, G.P., 2024. Global carbon budget 2024. *Earth System Science Data*  
928 *Discussions*, 2024, pp.1-133.  
929

930 Friedrichs, M.A., Dusenberry, J.A., Anderson, L.A., Armstrong, R.A., Chai, F., Christian, J.R., Doney, S.C.,  
931 Dunne, J., Fujii, M., Hood, R. and McGillicuddy Jr, D.J., 2007. Assessment of skill and portability in regional  
932 marine biogeochemical models: Role of multiple planktonic groups. *Journal of Geophysical Research: Oceans*,  
933 112(C8).  
934

935 Friedrichs, M.A.M., Carr, M.-E., Barber, R.T., Scardi, M., Antoine, D., Armstrong, R. A., *et al.* (2009) Assessing  
936 the uncertainties of model estimates of primary productivity in the tropical Pacific Ocean. *J. Mar. Syst.* 76, 113-  
937 133. doi:10.1016/j.jmarsys.2008.05.010  
938

939 Frölicher, T. L., K. B. Rodgers, C. A. Stock, and W. W. L. Cheung (2016), Sources of uncertainties in 21st century  
940 projections of potential ocean ecosystem stressors, *Global Biogeochem. Cycles*, 30, 1224–1243,  
941 doi:10.1002/2015GB005338.

942

943 Galli, G., Wakelin, S., Harle, J., Holt, J., Artioli, Y., 2024. Multi-model comparison of trends and controls of near-  
944 bed oxygen concentration on the northwest European continental shelf under climate change. *Biogeosciences* 21,  
945 2143–2158. <https://doi.org/10.5194/bg-21-2143-2024>

946

947 Garcia, H.E., Weathers, K.W., Paver, C.R., Smolyar, I., Boyer, T.P., Locarnini, M.M., Zweng, M.M., Mishonov,  
948 A.V., Baranova, O.K. and Seidov, D., 2019. World ocean atlas 2018. Vol. 4: Dissolved inorganic nutrients  
949 (phosphate, nitrate and nitrate+ nitrite, silicate).

950

951 Gastineau, G., & Soden, B. J. (2009). Model projected changes of extreme wind events in response to global  
952 warming. *Geophysical Research Letters*, 36(10). <https://doi.org/10.1029/2009GL037500>

953

954 Gattuso, J.P., Frankignoulle, M. and Wollast, R., 1998. Carbon and carbonate metabolism in coastal aquatic  
955 ecosystems. *Annual Review of Ecology and Systematics*, 29(1), pp.405-434.

956

957 Geider, RJ, Macintyre, HL, and Kana, TM (1997) Dynamic model of phytoplankton growth and acclimation:  
958 responses of the balanced growth rate and the chlorophyll a: carbon ratio to light, nutrient imitation and  
959 temperature,” *Mar. Ecol. Prog. Ser.* 148, 187–200.

960

961 Geider RJ, MacIntyre HL, Kana TM. (1998) A dynamic regulatory model of phytoplankton acclimation to light,  
962 nutrients, and temperatures. *Limnol. Oceanogr.*, 43(4), 679-694.

963

964 Gentile, E. S., Zhao, M., & Hodges, K. (2023). Poleward intensification of midlatitude extreme winds under  
965 warmer climate. *Npj Climate and Atmospheric Science*, 6(1), 1–10. <https://doi.org/10.1038/s41612-023-00540-x>

966

967 Gentleman, W., 2002. A chronology of plankton dynamics in silico: how computer models have been used to  
968 study marine ecosystems. *Hydrobiologia* 480, 69–85. DOI: 10.1023/A:1021289119442.

969

970 Gharamti ME, Samuelsen A, Bertino L, Simon E, Korosov A, Daewel U. Online tuning of ocean biogeochemical  
971 model parameters using ensemble estimation techniques: Application to a one-dimensional model in the North  
972 Atlantic. *Journal of Marine Systems*. 2017 Apr 1;168:1-6.

973

974 Gharamti ME, Tjiputra J, Bethke I, Samuelsen A, Skjelvan I, Bentsen M, Bertino L. Ensemble data assimilation  
975 for ocean biogeochemical state and parameter estimation at different sites. *Ocean Modelling*. 2017 Apr 1;112:65-  
976 89.

977

978 Gregg, W.W. and Rousseaux, C.S., 2016. Directional and spectral irradiance in ocean models: Effects on  
979 simulated global phytoplankton, nutrients, and primary production. *Frontiers in Marine Science*, 3, p.240.  
980

981 Gregg W.W and Rousseaux C.S. 2019. Global ocean primary production trends in the modern ocean color satellite  
982 record (1998–2015). *Environ. Res. Lett.* 14 124011  
983

984 Grégoire, M. and Soetaert, K., 2010. Carbon, nitrogen, oxygen and sulfide budgets in the Black Sea: A  
985 biogeochemical model of the whole water column coupling the oxic and anoxic parts. *Ecological Modelling*,  
986 221(19), pp.2287-2301.  
987

988 Grégoire, M., Raick, C. and Soetaert, K., 2008. Numerical modeling of the central Black Sea ecosystem  
989 functioning during the eutrophication phase. *Progress in Oceanography*, 76(3), pp.286-333.  
990

991 Grégoire, M. and Soetaert, K., 2010. Carbon, nitrogen, oxygen and sulfide budgets in the Black Sea: A  
992 biogeochemical model of the whole water column coupling the oxic and anoxic parts. *Ecological Modelling*,  
993 221(19), pp.2287-2301.  
994

995 Gulev, S.K., P.W. Thorne, J. Ahn, F.J. Dentener, C.M. Domingues, S. Gerland, D. Gong, D.S. Kaufman, H.C.  
996 Nnamchi, J. Quaas, J.A. Rivera, S. Sathyendranath, S.L. Smith, B. Trewin, K. von Schuckmann, and R.S. Vose,  
997 2021: Changing State of the Climate System. In *Climate Change 2021: The Physical Science Basis. Contribution*  
998 *of Working Group I to the Sixth Assessment Report of the Intergovernmental Panel on Climate Change* [Masson-  
999 Delmotte, V., P. Zhai, A. Pirani, S.L. Connors, C. Péan, S. Berger, N. Caud, Y. Chen, L. Goldfarb, M.I. Gomis,  
1000 M. Huang, K. Leitzell, E. Lonnoy, J.B.R. Matthews, T.K. Maycock, T. Waterfield, O. Yelekçi, R. Yu, and B.  
1001 Zhou (eds.)]. Cambridge University Press, Cambridge, United Kingdom and New York, NY, USA, pp. 287–422,  
1002 doi: 10.1017/9781009157896.004.  
1003

1004 Halsey, K.H., Milligan, A.J. and Behrenfeld, M.J., 2011. Linking time-dependent carbon-fixation efficiencies in  
1005 *Dunaliella Tertiolecta* (Chlorophyceae) to underlying metabolic pathways 1. *Journal of Phycology*, 47(1), pp.66-  
1006 76.  
1007

1008 Henson, S., Baker, C.A., Halloran, P., McQuatters-Gollop, A., Painter, S., Planchat, A. and Tagliabue, A., 2024.  
1009 Knowledge gaps in quantifying the climate change response of biological storage of carbon in the ocean. *Earth's*  
1010 *Future*, 12(6), p.e2023EF004375.  
1011

1012 Hewitt, C. D., and Coauthors, 2021: Recommendations for Future Research Priorities for Climate Modeling and  
1013 Climate Services. *Bull. Amer. Meteor. Soc.*, 102, E578–E588, <https://doi.org/10.1175/BAMS-D-20-0103.1>.  
1014

1015 IOCCG (2020). Synergy between Ocean Colour and Biogeochemical/Ecosystem Models. Dutkiewicz, S. (ed.),  
1016 IOCCG Report Series, No. 19, International Ocean Colour Coordinating Group, Dartmouth, Canada.  
1017 <http://dx.doi.org/10.25607/OBP-711>

1018

1019 IOCCG Protocol Series (2022). Aquatic Primary Productivity Field Protocols for Satellite Validation and Model  
1020 Synthesis. Balch, W.M., Carranza, M., Cetinić, I., Chaves, J.E., Duhamel, S., Fassbender, A., Fernandez-Carrera,  
1021 A., Ferrón, S., García-Martín, E., Goes, J., Gomes, H., Gundersen, K., Halsey, K., Hirawake, T., Isada, T., Juranek,  
1022 L., Kulk, G., Langdon, C., Letelier, R., López-Sandoval, D., Mannino, A., Marra, J.F., Neale, P., Nicholson, D.,  
1023 Silsbe, G., Stanley, R.H., Vandermeulen, R.A. IOCCG Ocean Optics and Biogeochemistry Protocols for Satellite  
1024 Ocean Colour Sensor Validation, Volume 7.0, edited by R.A. Vandermeulen, J. E. Chaves, IOCCG, Dartmouth,  
1025 NS, Canada. doi:<http://dx.doi.org/10.25607/OBP-1835>

1026

1027 IPCC (2019): IPCC Special Report on the Ocean and Cryosphere in a Changing Climate [H.-O. Pörtner, D.C.  
1028 Roberts, V. Masson-Delmotte, P. Zhai, M. Tignor, E. Poloczanska, K. Mintenbeck, A. Alegria, M. Nicolai, A.  
1029 Okem, J. Petzold, B. Rama, N.M. Weyer (eds.)].

1030

1031 IPCC, 2021: Climate Change 2021 - the Physical Science Basis, Contribution of Working Group I to the Sixth  
1032 Assessment Report of the Intergovernmental Panel on Climate Change [Masson-Delmotte, V., P. Zhai, A. Pirani,  
1033 S.L. Connors, C. Péan, S. Berger, N. Caud, Y. Chen, L. Goldfarb, M.I. Gomis, M. Huang, K. Leitzell, E. Lonnoy,  
1034 J.B.R. Matthews, T.K. Maycock, T. Waterfield, O. Yelekçi, R. Yu, and B. Zhou (eds.)]. Cambridge University  
1035 Press, In Press, Published: 9 August 2021.

1036

1037 Jackson, T, Sathyendranath, S, and T. Platt, T (2017) An exact solution for modeling photoacclimation of the  
1038 carbon-to-chlorophyll ratio in phytoplankton, *Front. Mar. Sci.* 4, 283

1039

1040 Jassby, A.D. and Platt, T., 1976. Mathematical formulation of the relationship between photosynthesis and light  
1041 for phytoplankton. *Limnology and oceanography*, 21(4), pp.540-547.

1042

1043 Jin, P., Hutchins, D.A. and Gao, K., 2020. The impacts of ocean acidification on marine food quality and its  
1044 potential food chain consequences. *Frontiers in Marine Science*, 7, p.543979.

1045

1046 Jones, C. G., Adloff, F., Booth, B., Cox, P., Eyring, V., Friedlingstein, P., Frieler, K., Hewitt, H., Jeffery, H.,  
1047 Jousaume, S., Koenigk, T., Lawrence, B. N., O'Rourke, E., Roberts, M., Sanderson, B., Séférian, R., Somot, S.,  
1048 Vidale, P.-L., van Vuuren, D., Acosta, M., Bentsen, M., Bernardello, R., Betts, R., Blockley, E., Boé, J.,  
1049 Bracegirdle, T., Braconnot, P., Brovkin, V., Buontempo, C., Doblus-Reyes, F. J., Donat, M. G., Epicoco, I.,  
1050 Falloon, P., Fiore, S., Froelicher, T., Fuckar, N., Gidden, M., Goessling, H., Graverson, R. G., Gualdi, S.,  
1051 Gutiérrez, J. M., Ilyina, T., Jacob, D., Jones, C., Juckes, M., Kendon, E., Kjellström, E., Knutti, R., Lowe, J. A.,  
1052 Mizieliński, M., Nassisi, P., Obersteiner, M., Regnier, P., Roehrig, R., Salas y Melia, D., Schleussner, C.-F.,  
1053 Schulz, M., Scoccimarro, E., Terray, L., Thiemann, H., Wood, R., Yang, S., and Zaehle, S.: Bringing it all  
1054 together: Science and modelling priorities to support international climate policy, *EGUsphere* [preprint],  
1055 <https://doi.org/10.5194/egusphere-2024-453>, 2024.

1056

1057 Kiefer, D.A. and Mitchell, B.G., 1983. A simple, steady state description of phytoplankton growth based on  
1058 absorption cross section and quantum efficiency 1. *Limnology and Oceanography*, 28(4), pp.770-776.  
1059

1060 Kim, H.H., Laufkötter, C., Lovato, T., Doney, S.C. and Ducklow, H.W., 2023. Projected 21st-century changes in  
1061 marine heterotrophic bacteria under climate change. *Frontiers in microbiology*, 14, p.1049579.  
1062

1063 Kishi, M.J., Kashiwai, M., Ware, D.M., Megrey, B.A., Eslinger, D.L., Werner, F.E., Noguchi-Aita, M., Azumaya,  
1064 T., Fujii, M., Hashimoto, S. and Huang, D., 2007. NEMURO—a lower trophic level model for the North Pacific  
1065 marine ecosystem. *Ecological Modelling*, 202(1-2), pp.12-25.  
1066

1067 Kovač, Ž., Platt, T., Sathyendranath, S., Morović, M., Jackson, T. (2016a). Recovery of photosynthesis parameters  
1068 from in situ profiles of phytoplankton production. *ICES Journal of Marine Science*, 73 (2), 275–285. DOI:  
1069 10.1093/icesjms/fsv204.  
1070

1071 Kovač, Ž., Platt, T., Sathyendranath, S., Morović, M. (2016b). Analytical solution for the vertical profile of daily  
1072 production in the ocean. *Journal of Geophysical Research: Oceans*, 121. DOI: 10.1002/2015JC011293.  
1073

1074 Kovač, Ž., Platt, T., S., S., Antunović, S. (2017). Models for estimating photosynthesis parameters from in situ  
1075 production profiles. *Progress in Oceanography*, 159, 255-266. doi:10.1016/j.pocean.2017.10.013.  
1076

1077 Kovač, Ž., Platt, T., Sathyendranath, S., Lomas, M. W. (2018). Extraction of photosynthesis parameters from time  
1078 series measurements of in situ production: Bermuda atlantic time-series study. *Remote Sensing*, 10, 915. DOI:  
1079 10.3390/rs10060915.  
1080

1081 Kovárová-Kovar, K. and Egli, T., 1998. Growth kinetics of suspended microbial cells: from single-substrate-  
1082 controlled growth to mixed-substrate kinetics. *Microbiology and molecular biology reviews*, 62(3), pp.646-666.  
1083

1084 Krinos, A.I., Shapiro, S.K., Li, W., Haley, S.T., Dyhrman, S.T., Dutkiewicz, S., Follows, M.J. and Alexander, H.  
1085 (2025), Intraspecific Diversity in Thermal Performance Determines Phytoplankton Ecological Niche. *Ecology*  
1086 *Letters*, 28: e70055. <https://doi.org/10.1111/ele.70055>  
1087

1088 Kulk, G, Platt, T, Dingle, J, Jackson, T, Jönsson, BF, Bouman, HA, Babin, M, Brewin, RJW, Doblin, M, Estrada,  
1089 M, Figueiras, FG, Furuya, K, González-Benítez, N, Gudfinnsson, HG, Gudmundsson, K, Huang, B, Isada, T,  
1090 Kovač, Ž, Lutz, VA, Marañón, E, Raman, M, Richardson, K, Rozema, PD, Poll, WH, Segura, V, Tilstone, GH,  
1091 Uitz, J, Dongen-Vogels, V, Yoshikawa, T, Sathyendranath, S (2020) Primary Production, an Index of Climate  
1092 Change in the Ocean: Satellite-Based Estimates over Two Decades. *Remote Sensing*, 12, 826.  
1093 <https://doi.org/10.3390/rs12050826>  
1094

1095 Kulk, G.; Platt, T.; Dingle, J.; Jackson, T.; Jönsson, B.F.; Bouman, H.A.; Babin, M.; Brewin, R.J.W.; Doblin, M.;  
1096 Estrada, M.; *et al.* Correction: Kulk *et al.* Primary Production, an Index of Climate Change in the Ocean: Satellite-

1097 Based Estimates over Two Decades. *Remote Sens.* 2020, 12, 826. *Remote Sens.* 2021, 13, 3462.  
1098 <https://doi.org/10.3390/rs13173462>  
1099

1100 Kyewalyanga, M., Platt, T., & Sathyendranath, S. (1992). Ocean primary production calculated by spectral and  
1101 broadband models. *Marine Ecology Progress Series*, 85, 171–185. DOI: 10.3354/meps085171.  
1102

1103 Kyewalyanga, MN, Platt, T, Sathyendranath, S (1997) Estimation of the photosynthetic action spectrum:  
1104 implications for primary production models. *Mar. Ecol. Prog. Ser.* 146: 207-223.  
1105

1106 Kwiatkowski, L., Bopp, L., Aumont, O., Ciais, P., Cox, P.M., Laufkötter, C., Li, Y. and Séférian, R., 2017.  
1107 Emergent constraints on projections of declining primary production in the tropical oceans. *Nature Climate*  
1108 *Change*, 7(5), pp.355-358.  
1109

1110 Kwiatkowski, L., Torres, O., Bopp, L., Aumont, O., Chamberlain, M., Christian, J.R., Dunne, J.P., Gehlen, M.,  
1111 Ilyina, T., John, J.G., Lenton, A., Li, H., Lovenduski, N.S., Orr, J.C., Palmieri, J., Santana-Falcón, Y., Schwinger,  
1112 J., Séférian, R., Stock, C.A., Tagliabue, A., Takano, Y., Tjiputra, J., Toyama, K., Tsujino, H., Watanabe, M.,  
1113 Yamamoto, A., Yool, A., Ziehn, T., 2020. Twenty-first century ocean warming, acidification, deoxygenation, and  
1114 upper-ocean nutrient and primary production decline from CMIP6 model projections. *Biogeosciences* 17, 3439–  
1115 3470. <https://doi.org/10.5194/bg-17-3439-2020>  
1116

1117 Laufkötter, C., Vogt, M., Gruber, N., Aita-Noguchi, M., Aumont, O., Bopp, L., Buitenhuis, E., Doney, S. C.,  
1118 Dunne, J., Hashioka, T., Hauck, J., Hirata, T., John, J., Le Quééré, C., Lima, I. D., Nakano, H., Seferian, R.,  
1119 Totterdell, I., Vichi, M., and Völker, C. (2015) Drivers and uncertainties of future global marine primary  
1120 production in marine ecosystem models, *Biogeosciences*, 12, 6955–6984, [https://doi.org/10.5194/bg-12-6955-](https://doi.org/10.5194/bg-12-6955-2015)  
1121 2015  
1122

1123 Lee, Z. Veronica P. Lance, VP, Shang, S, Vaillancourt,R, Freeman,S, Lubac, B, Hargreaves, BR, Del Castillo, C,  
1124 Richard Miller, R, Twardowski, M, Wei, G (2011) An assessment of optical properties and primary production  
1125 derived from remote sensing in the Southern Ocean (SO GasEx). *J. Geophys. Res.* 116, C00F03 (2011).  
1126 doi:10.1029/2010JC006747.  
1127

1128 Lee Z, Marra J, Perry MJ, Kahru M (2015). Estimating oceanic primary productivity from ocean color remote  
1129 sensing: A strategic assessment, *Journal of Marine Systems*. <http://dx.doi.org/10.1016/j.jmarsys.2014.11.015>Lee,  
1130 S. and Yoo, S. (2016) ‘Interannual variability of the phytoplankton community by the changes in vertical mixing  
1131 and atmospheric deposition in the Ulleung Basin, East Sea: A modelling study’, *Ecological Modelling*, 322, pp.  
1132 31–47. Available at: <https://doi.org/10.1016/j.ecolmodel.2015.11.012>.  
1133

1134 Lee, Y. J., P. A. Matrai, M. A. M. Friedrichs, V. S. Saba, D. Antoine, M. Ardyna, I. Asanuma, M. Babin, S.  
1135 Belanger, M. Benoit-Gagne, E. Devred, M. Fernandez-Mendez, B. Gentili, T. Hirawake, S.-H. Kang, T. Kameda,  
1136 C. Katlein, S.H. Lee, Z. Lee, F. Melin, M. Scardi, T.J. Smyth, S. Tang, K.R. Turpie, K.J. Waters, and T.K.

1137 Westberry (2015). An assessment of ocean color model estimates of primary productivity in the Arctic Ocean. *J.*  
1138 *Geophys. Res. Oceans*, FAMOS SI, 120:6508–6541, DOI 10.1002/2015JC011018.  
1139

1140 Liu, H., Li, D., Chen, Q., Feng, J., Qi, J., & Yin, B. (2024). The multiscale variability of global extreme wind and  
1141 wave events and their relationships with climate modes. *Ocean Engineering*, 307, 118239.  
1142 <https://doi.org/10.1016/j.oceaneng.2024.118239>  
1143

1144 Longhurst, A, Sathyendranath, S, Platt, T, Caverhill, C (1995) An estimate of global primary production in the  
1145 ocean from satellite radiometer data. *J. Plankton Res.* 17: 1245-1271.  
1146

1147 Longhurst, A.R. *Ecological Geography of the Sea*, 2nd ed.; Elsevier Academic Press: Cambridge, MA, USA,  
1148 2007; p. 542.  
1149

1150 Löptien, U. and Dietze, H., 2019. Reciprocal bias compensation and ensuing uncertainties in model-based climate  
1151 projections: pelagic biogeochemistry versus ocean mixing. *Biogeosciences*, 16(9), pp.1865-1881.  
1152

1153 Lurin, B., Rasool, S.I., Cramer, W. and Moore, B. (1994) Global terrestrial net primary production. *Glob. Change*  
1154 *NewsL (IGBP)*, 19, 6-8.  
1155

1156 Luypaert, T., Hagan, J.G., McCarthy, M.L. and Poti, M., 2020. Status of marine biodiversity in the  
1157 Anthropocene. *YOUMARES*, 9, pp.57-82.  
1158

1159 Maishal, S., 2024. Decadal changes in global Oceanic Primary Productivity and its drivers. *Ocean-Land-*  
1160 *Atmosphere Research*, 3, p.0066.  
1161

1162 Marshak, A.R., Link, J.S. Primary production ultimately limits fisheries economic performance. *Sci Rep* 11,  
1163 12154 (2021). <https://doi.org/10.1038/s41598-021-91599-0>  
1164

1165 Mattern J P., Fennel K., Dowd M. (2012). Estimating time-dependent parameters for a biological ocean model  
1166 using an emulator approach. *J. Mar. Syst.* 96, 32–47. doi: 10.1016/j.jmarsys.2012.01.015.  
1167 Michaelis L, Menten ML. Die kinetik der invertinwirkung. *Biochem. z.* 1913 Feb;49(333-369):352.  
1168

1169 Mitra, A., Caron, D.A., Faure, E., Flynn, K.J., Leles, S.G., Hansen, P.J., McManus, G.B., Not, F., do Rosario  
1170 Gomes, H., Santoferrara, L.F. and Stoecker, D.K., 2023. The Mixoplankton Database (MDB): Diversity of photo-  
1171 phago-trophic plankton in form, function, and distribution across the global ocean. *Journal of Eukaryotic*  
1172 *Microbiology*, 70(4), p.e12972.  
1173

1174 Myksovoll, M.S., Sandø, A.B., Tjiputra, J., Samuelsen, A., Yumruktepe, V.Ç., Li, C., Mousing, E.A., Bettencourt,  
1175 J.P. and Ottersen, G., 2023. Key physical processes and their model representation for projecting climate impacts  
1176 on subarctic Atlantic net primary production: A synthesis. *Progress in Oceanography*, 217, p.103084.

1177

1178 Norberg J., Biodiversity and ecosystem functioning: A complex adaptive systems approach, *Limnology and*  
1179 *Oceanography*, 4, part 2, doi: 10.4319/lo.2004.49.4\_part\_2.1269. 2004.

1180

1181 T. Parsons, M. Takahashi, B. Hargrave., *Biological Oceanographic Processes* (Third edition), Pergamon  
1182 International Library of Science, Technology, Engin, Pergamon (1984)

1183

1184 Pastres, R., Ciavatta, S. and Solidoro, C., 2003. The Extended Kalman Filter (EKF) as a tool for the assimilation  
1185 of high frequency water quality data. *Ecological modelling*, 170(2-3), pp.227-235.

1186

1187 Platt, T., Gallegos, C.L. and Harrison, W.G., 1980. Photoinhibition of photosynthesis in natural assemblages of  
1188 marine phytoplankton.

1189

1190 Platt, T., Sathyendranath, S (1988) Oceanic primary production: Estimation by remote sensing at local and  
1191 regional scales. *Science* 241: 1613-1620.

1192

1193 Platt, T., Sathyendranath, S, Ravindran, P (1990) Primary production by phytoplankton: analytic solutions for  
1194 daily rates per unit area of water surface. *Proc. R. Soc. Lond. Ser. B* 241: 101-111.

1195

1196 Platt, T, Sathyendranath, S (1991) Biological production models as elements of coupled, atmosphere-ocean  
1197 models for climate research. *J. Geophys. Res.* 96: 2585-2592.

1198

1199 Platt, T, Sathyendranath, S (1993) Estimators of primary production for interpretation of remotely sensed data on  
1200 ocean color. *J. Geophys. Res.* 98: 14,561-14,576.

1201 Platt, T, Sathyendranath, S (1997) Modelling primary production IV (in Japanese). *Aquabiology* 19: 229-232.

1202

1203 Radtke, H., Lipka, M., Bunke, D., Morys, C., Woelfel, J., Cahill, B., Böttcher, M.E., Forster, S., Leipe, T., Rehder,  
1204 G. and Neumann, T., 2019. Ecological ReGional Ocean Model with vertically resolved sediments (ERGOM SED  
1205 1.0): coupling benthic and pelagic biogeochemistry of the south-western Baltic Sea. *Geoscientific Model*  
1206 *Development*, 12(1), pp.275-320.

1207

1208 Ratnarajah L, Abu-Alhaja R, Atkinson A, Batten S, Bax NJ, Bernard KS, Canonico G, Cornils A, Everett JD,  
1209 Grigoratou M, Ishak NH. Monitoring and modelling marine zooplankton in a changing climate. *Nature*  
1210 *Communications*. 2023 Feb 2;14(1):564.

1211

1212 Regaudie-de-Gioux, A., Lasternas, S., Agustí, S., Duarte, C.M. 2019. Comparing marine primary production  
1213 estimates through different methods and development of conversion equations. *Frontiers in Marine Science*, 1.  
1214 URL: <https://www.frontiersin.org/journals/marine-science/articles/10.3389/fmars.2014.00019>. DOI=10.3389/  
1215 fmars.2014.00019

1216

1217 Rohr T, Richardson AJ, Lenton A, Chamberlain MA, Shadwick EH. Zooplankton grazing is the largest source of  
1218 uncertainty for marine carbon cycling in CMIP6 models. *Communications Earth & Environment*. 2023 Jun  
1219 14;4(1):212.  
1220

1221 Roy S, Broomhead DS, Platt T, Sathyendranath S, Ciavatta S. Sequential variations of phytoplankton growth and  
1222 mortality in an NPZ model: A remote-sensing-based assessment. *Journal of Marine Systems*. 2012 Apr  
1223 1;92(1):16-29.  
1224

1225 Ryan-Keogh, T.J., Tagliabue, A. & Thomalla, S.J. Global decline in net primary production underestimated by  
1226 climate models. *Commun Earth Environ* **6**, 75 (2025). <https://doi.org/10.1038/s43247-025-02051-4>  
1227

1228 Saba, V.S., Friedrichs, M.A.M., Carr, M.-E., Antoine, D., Armstrong, R.A., Asanuma, I., *et al.*(2010) Challenges  
1229 of modeling depth-integrated marine primary productivity over multiple decades: a case study at BATS and HOT.  
1230 *Glob. Biogeochem. Cycle* **24**, GB3020.[doi:10.1029/2009GB003655](https://doi.org/10.1029/2009GB003655)  
1231

1232 Sathyendranath, S., & Platt, T. (1989a). Computation of aquatic primary production: Extended formalism to  
1233 include the effect of angular and spectral distribution of light. *Limnology and Oceanography*, **34**, 188–198. DOI:  
1234 [10.4319/lo.1989.34.1.0188](https://doi.org/10.4319/lo.1989.34.1.0188).  
1235

1236 Sathyendranath, S, Platt, T, Caverhill, CM, Warnock, RE, Lewis, MR (1989b) Remote sensing of oceanic primary  
1237 production: Computations using a spectral model. *Deep-Sea Res. I* **36**: 431-453.  
1238

1239 Sathyendranath, S, Platt, T (2007) Spectral effects in bio-optical control on the ocean system. *Oceanologia* **49**: 5-  
1240 39.  
1241

1242 Sathyendranath, S, Stuart, V, Nair, A, Oka, K., Nakane, T, Bouman, H, Forget, M-H, Maass, H, Platt, T (2009)  
1243 Carbon-to-chlorophyll ratio and growth rate of phytoplankton in the sea. *Mar. Ecol. Prog. Ser.* **383**: 73–84, doi:  
1244 [10.3354/meps07998](https://doi.org/10.3354/meps07998)  
1245

1246 Sathyendranath, S., Brewin, R., Brockmann, C., Brotas, V., Calton, B., Chuprin, A., *et al.* (2019). An ocean-  
1247 colour time series for use in climate studies: The experience of the Ocean-Colour Climate Change Initiative (OC-  
1248 CCI). *Sensors*, **19**(19), 4285. <https://doi.org/10.3390/s19194285>  
1249

1250 Sathyendranath, S, Platt, T, Kovač, Ž, Dingle, J, Jackson, T, Brewin, R JW, Franks, P, Marañón, E, Kulk, G, and  
1251 Bouman, HA (2020) Reconciling models of primary production and photoacclimation [Invited]. *Applied Optics*,  
1252 **59**: C100-C114. <https://doi.org/10.1364/AO.386252>  
1253

1254 Sathyendranath, S., Brewin, R.J.W., Ciavatta, S. Jackson, T., Kulk, G., Jönsson, B. Martinez Vicente, V, Platt, T.  
1255 (2023) Ocean Biology Studied from Space. *Surv Geophys* **44**, 1287–1308. [https://doi.org/10.1007/s10712-023-](https://doi.org/10.1007/s10712-023-09805-9)  
1256 [09805-9](https://doi.org/10.1007/s10712-023-09805-9)

1257

1258 Sauterey B., Le Gland G., Cermeño P., Aumont O., Lévy M., Vallina S.M., Phytoplankton adaptive resilience to  
1259 climate change collapses in case of extreme events – A modeling study. *Ecological Modelling*, Volume 483, 2023,  
1260 110437, ISSN 0304-3800, <https://doi.org/10.1016/-j.ecolmodel.2023.110437>

1261

1262 Séférian, R., Berthet, S., Yool, A., Palmiéri, J., Bopp, L., Tagliabue, A., Kwiatkowski, L., Aumont, O., Christian,  
1263 J., Dunne, J., Gehlen, M., Ilyina, T., John, J.G., Li, H., Long, M.C., Luo, J.Y., Nakano, H., Romanou, A.,  
1264 Schwinger, J., Stock, C., Santana-Falcón, Y., Takano, Y., Tjiputra, J., Tsujino, H., Watanabe, M., Wu, T., Wu,  
1265 F., Yamamoto, A., 2020. Tracking Improvement in Simulated Marine Biogeochemistry Between CMIP5 and  
1266 CMIP6. *Curr Clim Change Rep* 6, 95–119. <https://doi.org/10.1007/s40641-020-00160-0>

1267

1268 Schartau, M., Wallhead, P., Hemmings, J., Löptien, U., Kriest, I., Krishna, S., Ward, B. A., Slawig, T., and  
1269 Oschlies, A.: Reviews and syntheses: parameter identification in marine planktonic ecosystem modelling,  
1270 *Biogeosciences*, 14, 1647–1701, <https://doi.org/10.5194/bg-14-1647-2017>, 2017.

1271

1272 Schmidtko S., Stramma L., Visbeck M. (2017). Decline in global oceanic oxygen content during the past five  
1273 decades. *Nature* 542, 335–339. doi: 10.1038/nature21399

1274

1275 Shigemitsu, M., Okunishi, T., Nishioka, J., Sumata, H., Hashioka, T., Aita, M.N., Smith, S.L., Yoshie, N., Okada,  
1276 N. and Yamanaka, Y., 2012. Development of a one-dimensional ecosystem model including the iron cycle applied  
1277 to the Oyashio region, western subarctic Pacific. *Journal of Geophysical Research: Oceans*, 117(C6).

1278

1279 Silsbe, G.M., Behrenfeld, M.J., Halsey, K.H., Milligan, A.J. and Westberry, T.K., 2016. The CAFE model: A net  
1280 production model for global ocean phytoplankton. *Global Biogeochemical Cycles*, 30(12), pp.1756-1777.

1281

1282 Silsbe, G.M., Fox, J., Westberry, T.K. *et al.* Global declines in net primary production in the ocean color era. *Nat*  
1283 *Commun* 16, 5821 (2025). <https://doi.org/10.1038/s41467-025-60906-y>

1284

1285 Simon E, Samuelsen A, Bertino L, Mouysset S. Experiences in multiyear combined state–parameter estimation  
1286 with an ecosystem model of the North Atlantic and Arctic Oceans using the Ensemble Kalman Filter. *Journal of*  
1287 *Marine Systems*. 2015 Dec 1;152:1-7.

1288

1289 Singh, T., Counillon, F., Tjiputra, J. and Wang, Y., 2025. A novel ensemble-based parameter estimation for  
1290 improving ocean biogeochemistry in an Earth system model. *Journal of Advances in Modeling Earth*  
1291 *Systems*, 17(2), p.e2024MS004237.

1292

1293 Skákala, J., Wakamatsu, T., Bertino, L., Teruzzi, A., Lazzari, P., Alvarez, E., Cossarini, G., Spada, S., Nerger, L.,  
1294 Vliegen, S., Brankart, J. M., and Brasseur, P.: SEAMLESS Target indicator quality in CMEMS MFCs (D6.1),  
1295 <https://doi.org/10.5281/zenodo.10522305>, 2024.

1296

1297 Smith, S.L., Yamanaka, Y., Pahlow, M. and Oschlies, A., 2009. Optimal uptake kinetics: physiological  
1298 acclimation explains the pattern of nitrate uptake by phytoplankton in the ocean. *Marine Ecology Progress Series*,  
1299 384, pp.1-12.  
1300

1301 Steele, J.H., 1962. Environmental control of photosynthesis in the sea. *Limnology and oceanography*, 7(2),  
1302 pp.137-150.  
1303

1304 Steele, J.H, Henderson, E.W. (1992) The role of predation in plankton models. *Journal of Plankton Research*,  
1305 14(1): 157-172.  
1306

1307 Steinacher, M., Joos, F., Frölicher, T. L., Bopp, L., Cadule, P., Cocco, V., Doney, S. C., Gehlen, M., Lindsay, K.,  
1308 Moore, J. K., Schneider, B., and Segschneider, J.: Projected 21st century decrease in marine productivity: a multi-  
1309 model analysis, *Biogeosciences*, 7, 979–1005, <https://doi.org/10.5194/bg-7-979-2010>, 2010  
1310

1311 Stock, C.A., Dunne, J.P., Fan, S., Ginoux, P., John, J., Krasting, J.P., Laufkötter, C., Paulot, F. and Zadeh, N.,  
1312 2020. Ocean biogeochemistry in GFDL's Earth System Model 4.1 and its response to increasing atmospheric CO<sub>2</sub>.  
1313 *Journal of Advances in Modeling Earth Systems*, 12(10), p.e2019MS002043.  
1314

1315 Stock, C.A., Dunne, J.P., Luo, J.Y., Ross, A.C., Van Oostende, N., Zadeh, N., Cordero, T.J., Liu, X. and Teng,  
1316 Y.C., 2025. Photoacclimation and photoadaptation sensitivity in a global ocean ecosystem model. *Journal of*  
1317 *Advances in Modeling Earth Systems*, 17(6), p.e2024MS004701.  
1318

1319 Stock, C.A., 2019. Comparing apples to oranges: Perspectives on satellite-based primary production estimates  
1320 drawn from a global biogeochemical model, *Journal of Marine Research*, 77, (S). [https://elischolar.library.yale-](https://elischolar.library.yale.edu/journal_of_marine_research/480)  
1321 [.edu/journal\\_of\\_marine\\_research/480](https://elischolar.library.yale.edu/journal_of_marine_research/480).  
1322

1323 Tagliabue A, Kwiatkowski L, Bopp L, Butenschön M, Cheung W, Lengaigne M and Vialard J (2021) Persistent  
1324 Uncertainties in Ocean Net Primary Production Climate Change Projections at Regional Scales Raise Challenges  
1325 for Assessing Impacts on Ecosystem Services. *Front. Clim.* 3:738224. doi: 10.3389/fclim.2021.738224  
1326

1327 Tao, Zui & Wang, Yan & Ma, Sheng & Lv, Tingting & Zhou, Xiang. (2017). A Phytoplankton Class-Specific  
1328 Marine Primary Productivity Model Using MODIS Data. *IEEE Journal of Selected Topics in Applied Earth*  
1329 *Observations and Remote Sensing*. PP. 1-10. 10.1109/JSTARS.2017.2747770.  
1330

1331 Tjiputra, J.F., Polzin, D. and Winguth, A.M., 2007. Assimilation of seasonal chlorophyll and nutrient data into an  
1332 adjoint three-dimensional ocean carbon cycle model: Sensitivity analysis and ecosystem parameter  
1333 optimization. *Global biogeochemical cycles*, 21(1).  
1334

1335 Tjiputra, J.F., Couespel, D. and Sanders, R., 2025. Marine ecosystem role in setting up preindustrial and future  
1336 climate. *Nature Communications*, 16(1), p.2206.

1337

1338 Thomas, M.K., Kremer, C.T. and Litchman, E. (2016), Phytoplankton temperature trait biogeography. *Global*  
1339 *Ecology and Biogeography*, 25: 75-86. <https://doi.org/10.1111/geb.12387>

1340

1341 Uitz J, Claustre H, Gentili B, Stramski D. (2010). Phytoplankton class-specific primary production in the world's  
1342 oceans: Seasonal and interannual variability from satellite observations. *Global Biogeochemical Cycles* 24.  
1343 <https://doi.org/10.1029/2009GB003680>

1344

1345 Vichi, M., Pinardi, N. and Masina, S., 2007. A generalized model of pelagic biogeochemistry for the global ocean  
1346 ecosystem. Part I: Theory. *Journal of Marine Systems*, 64(1-4), pp.89-109.

1347

1348 Ward, B.A., Dutkiewicz, S., Jahn, O. and Follows, M.J., 2012. A size-structured food-web model for the global  
1349 ocean. *Limnology and Oceanography*, 57(6), pp.1877-1891.

1350

1351 Webb, W.L., Newton, M. and Starr, D., 1974. Carbon dioxide exchange of *Alnus rubra*: a mathematical model.  
1352 *Oecologia*, 17, pp.281-291

1353

1354 Westberry, T., Behrenfeld, M.J., Siegel, D.A. and Boss, E., 2008. Carbon-based primary productivity modeling  
1355 with vertically resolved photoacclimation. *Global Biogeochemical Cycles*, 22(2).

1356

1357 Wu, Z., S. Dutkiewicz., O. Jahn, D. Sher, A. White, and M.J. Follows, 2021. Modeling photosynthesis and  
1358 exudation in the subtropical oceans. *Global Biogeochemical Cycles*, 35, doi:10.1029/2021GB006941

1359

1360 Xiao, Y. and Friedrichs, M.A., 2014. Using biogeochemical data assimilation to assess the relative skill of multiple  
1361 ecosystem models in the Mid-Atlantic Bight: effects of increasing the complexity of the planktonic food web.  
1362 *Biogeosciences*, 11(11), pp.3015-3030.

1363

1364 Yool, A., Popova, E.E. and Anderson, T.R., 2013. MEDUSA-2.0: an intermediate complexity biogeochemical  
1365 model of the marine carbon cycle for climate change and ocean acidification studies. *Geoscientific Model*  
1366 *Development*, 6(5), pp.1767-1811.

1367

1368 Young, I. R., & Ribal, A. (2019). Multiplatform evaluation of global trends in wind speed and wave height.  
1369 *Science*, 364(6440), 548–552. <https://doi.org/10.1126/science.aav9527>

1370

1371 Yumruktepe, V.Ç., Samuelsen, A. and Daewel, U., 2022. ECOSMO II (CHL): a marine biogeochemical model  
1372 for the North Atlantic and the Arctic. *Geoscientific Model Development*, 15(9), pp.3901-3921.

1373

1374 Zheng, Q., Viljoen, J.J., Sun, X., Kovač, Ž., Sathyendranath, S. and Brewin, R.J., 2025. Simulating vertical  
1375 phytoplankton dynamics in a stratified ocean using a two-layered ecosystem model. *Biogeosciences*, 22(13),  
1376 pp.3253-3278.

